Text and references accompanying Nevada Bureau of Mines and Geology Map 183

Geologic Map of the Southern Part of the Eureka Mining District and Surrounding Areas of the Fish Creek Range, Mountain Boy Range, and Diamond Mountains, Eureka and White Pine Counties, Nevada

by

Sean P. Long[1], Christopher D. Henry[1], John L. Muntean[1],
Gary P. Edmondo[2], and Robert D. Thomas[3]

[1]Nevada Bureau of Mines and Geology, University of Nevada, Reno
[2]Timberline Resources Corporation, Coeur d'Alene, ID
[3]Consulting Geologist

2014

INTRODUCTION

The Eureka mining district is located in east-central Nevada, within the northern part of the Fish Creek Range (fig. 1). The Eureka mining district is in many ways the birthplace of Great Basin geology. Studies by USGS geologists as early as the 1880s (Curtis, 1884; Hague, 1892; Walcott, 1884) laid the foundation for understanding the Paleozoic stratigraphic section, and were the first to document the presence of carbonate-hosted silver-gold-lead replacement ores. An extensive geologic resurvey of the district and surrounding region by the USGS that began in the 1930s resulted in classic studies that define Paleozoic stratigraphy (Nolan et al., 1956; Palmer, 1960; Brew, 1961a; 1961b; 1971; Nolan, 1962; Stewart, 1962; Ross, 1970), and geologic maps of the Eureka and Pinto Summit 15-minute quadrangles (Nolan et al., 1971; 1974).

Early geologic mapping (Nolan, 1962; Nolan et al., 1971; 1974) showed that the Eureka region occupies a zone of thrust-faults and folds, which was later interpreted as part of the central Nevada thrust belt (Taylor et al., 1993), a north-trending system of Mesozoic-age contractional structures that represents an interior component of the Sevier fold-thrust belt (e.g., Taylor et al., 2000; Long, 2012). However, there has been significant variation in interpretations of the style and geometry of large-offset structures in different generations of studies in the Eureka region (e.g., Nolan, 1962; Nolan et al., 1974; Taylor et al., 1993; Lisenbee et al., 1995; Long et al., 2014), and these varying interpretations are compounded by the effects of complex, overprinting extensional deformation. This has hindered accurate representation of the regional structural geometry, and interpretation of the timing, magnitude, and genesis of superposed contractional and extensional deformation events. In addition to varying interpretations of the tectonic history, the genesis, age, and regional significance of mid-Tertiary silicic and intermediate volcanic rocks in the Eureka region, referred to here as the Eureka volcanic center, are to date poorly understood. Previous mapping by Nolan et al. (1971; 1974) was hindered by less-accurate K-Ar age dating, which allowed these volcanic rocks to only be generally characterized.

To address these problems, we present a new 1:24,000-scale transect geologic map, which covers an area ca. 25 km east-west by ca. 7 km north-south (fig. 1). The map trends through the northern Fish Creek Range, southern Mountain Boy Range, and southern Diamond Mountains, and passes through the southern part of the Eureka mining district (fig. 1). This effort consisted of 1) new mapping in the Fish Creek and Mountain Boy ranges, 2) new mapping combined with compilation and field checking of unpublished 1:1,200-scale mapping performed in the southern part of the district by Timberline Resources Corporation, and 3) compilation and field-checking of 1:31,680-scale mapping in the southern Diamond Mountains by Nolan et al. (1974). In addition, three 1:24,000-scale cross sections are presented, which illustrate the deformation geometry both above and below the modern erosion surface. This map and report are meant to accompany Long et al. (2014), which quantifies extension and shortening magnitudes, brackets the timing of contractional and extensional events, and presents a geometric model for deformation in the map area.

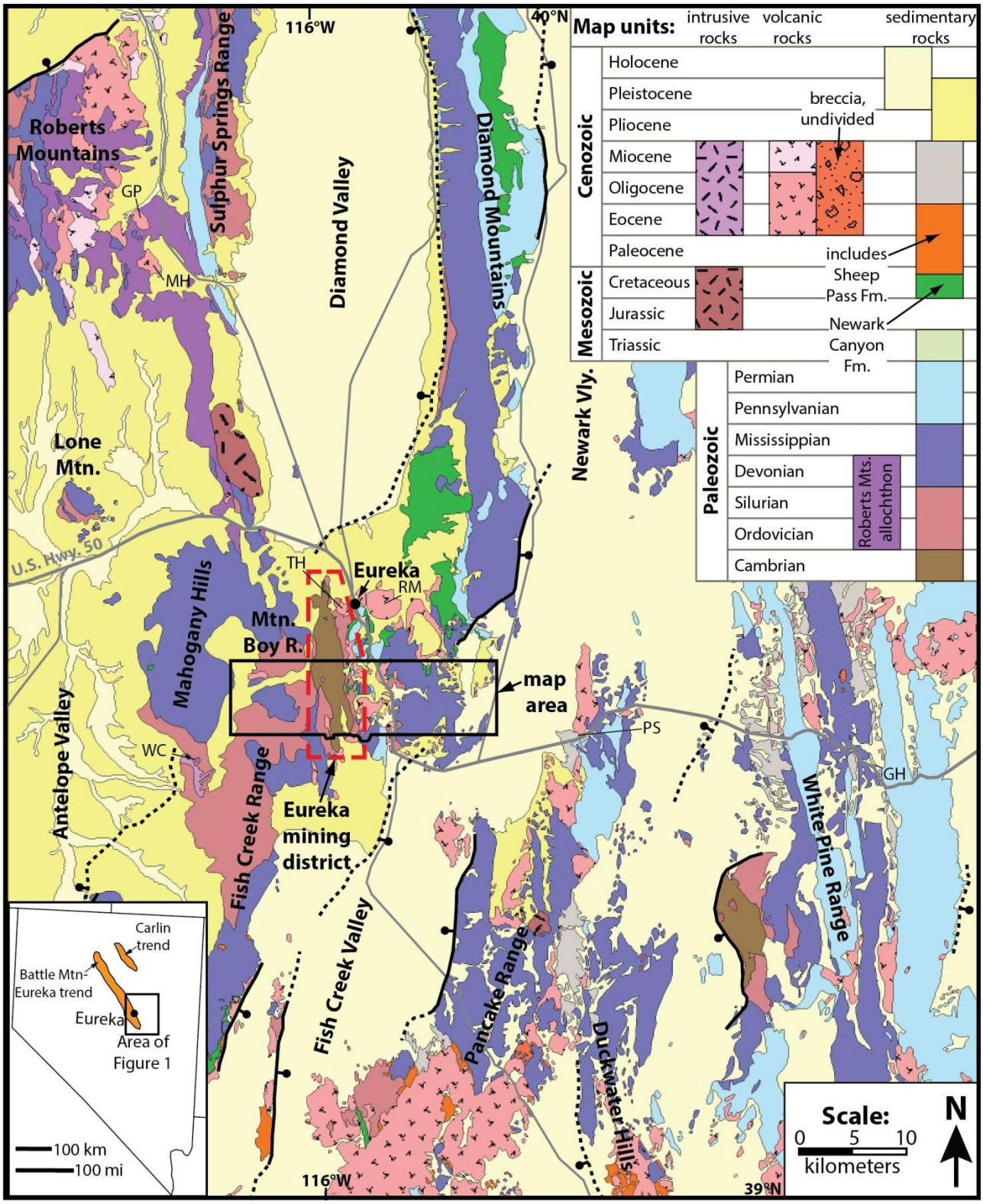

Figure 1. Geologic map of part of east-central Nevada, modified from Long et al. (2014); geology simplified from Crafford (2007) and Quaternary faults simplified from the USGS fault and fold database (2006). Outline of map area and approximate outline of Eureka mining district are shown. Lower left inset shows location relative to Battle Mountain–Eureka and Carlin mineral trends. Abbreviations: GP = Garden Pass, MH = Mount Hope, WC = Wood Cone Peak, PS = Pancake Summit, GH = Garnet Hill, TH = Target Hill, RM = Richmond Mountain.

In summary, in this map and report, we: 1) describe stratigraphy in a classic location of Paleozoic strata; 2) document the distribution, petrographic and chemical characteristics, and timing of the Eureka volcanic center, and compare it with other Eocene igneous centers in the region; 3) explain significant revisions to the stratigraphy and structure; 4) describe mineral deposits in the map area, and 5) summarize the geologic history of the Eureka area.

STRATIGRAPHY

A cumulative thickness of ca. 7.5 km of Cambrian to Permian sedimentary rocks is exposed in the map area. The Cambrian to Devonian section is typical of the Cordilleran passive margin basin (e.g., Stewart and Poole, 1974), and is dominated by limestone and dolomite, with lesser quartzite and shale. The Mississippian section consists of conglomerate, sandstone, and shale deposited in the Antler foreland basin (e.g., Poole, 1974) and the overlying Antler successor basin (Trexler et al., 2003), and the Pennsylvanian and Permian section is comprised of limestone and conglomerate.

Mesozoic rocks include the Early Cretaceous Newark Canyon Formation, which is only preserved in the northeast part of the map area, lying unconformably over Mississippian and Pennsylvanian rocks. The Newark Canyon Formation type-exposure is located ca. 1–5 km north of the map area (Nolan et al. 1971; 1974) (fig. 1). In addition, a conglomerate unit exposed on Hoosac Mountain, which unconformably overlies Ordovician, Mississippian, and Permian rocks, is bracketed between Late Cretaceous and late Eocene (Long et al., 2014).

Tertiary rocks in the map area consist of late Eocene silicic lava flows and domes, tuffs, shallow intrusions, and associated volcaniclastic and sedimentary rocks. Igneous rocks of the ca. 37.4–35.4 Ma Eureka volcanic center are discussed in the next section. Younger volcanic rocks in the map area, unrelated to the Eureka volcanic center (fig. 2), are confined to Rescue Canyon, where Eocene and Oligocene (ca. 35 and ca. 25 Ma) ash-flow tuffs and early Miocene (ca. 20 Ma) basalt are present (Nolan et al., 1974).

Quaternary deposits, including alluvial fans, alluvium, and colluvium, are also mapped. Kilometer-scale alluvial fan systems form alluvial aprons in several areas bounding modern topographic basins, including Spring Valley in the northwest part of the map area, and the eastern flank of the Diamond Mountains. Colluvium is particularly common on slopes below exposures of well-indurated Paleozoic rocks such as the Eureka quartzite, and on slopes below poorly-indurated Tertiary volcanic and sedimentary rocks.

CENOZOIC IGNEOUS ROCKS AND MAGMATISM OF THE EUREKA VOLCANIC CENTER

Dacite, rhyolite, and andesite intruded and erupted in five episodes between ~37.4 and 35.4 Ma. The episodes are distinguished on the basis of stratigraphy, rock type, and $^{40}Ar/^{39}Ar$ dates (fig. 2, table 1). Our work on Cenozoic igneous rocks builds upon that of Nolan et al. (1956, 1971, 1974), Nolan (1962), and Blake et al. (1975). Blake et al. (1975) synthesized various informal and formal names into three major formations of locally-derived igneous rocks of the Eureka volcanic center. From youngest to oldest, they are the Richmond Mountain Andesite, Pinto Peak Rhyolite (with two named tuff members), and Ratto Spring Rhyodacite. In this discussion, we mostly retain these names, we add the Target Hill rhyolite because our new mapping, petrographic and geochemical analyses, and precise $^{40}Ar/^{39}Ar$ dating show that the original Pinto Peak Rhyolite includes rocks of two distinct ages, ~35.9 Ma (Target Hill rhyolite) and ~36.6 Ma (Pinto Peak Rhyolite) (table 1), and we divide the Richmond Mountain Andesite into the Richmond Mountain dacite (~36.2 Ma) and Basalt Peak andesite (~35.5 Ma).

Interbedding or cross-cutting relations between igneous rocks are sparse because they erupted onto a surface with major topographic relief, most igneous rocks did not flow significant lateral distances, and many are shallow intrusions. Therefore, precise $^{40}Ar/^{39}Ar$ dates are essential for resolving the overall igneous evolution.

Published Isotopic Ages of Cenozoic Rocks

Numerous K-Ar dates for Eureka district rocks establish that Cenozoic igneous activity occurred at ~35–36 Ma (Nolan et al., 1974; Blake et al., 1975). Corrected for modern decay constants, individual dates range from ~34 to 39 Ma. Where we can be reasonably certain of K-Ar sample locations, similar, related, or nearby samples variably do or do not match our dates. Two biotite K-Ar dates of rocks likely sampled in the Rustler pit are 37.3±1.3 Ma on an andesite-dacite intrusive rock and 39.0±0.8 Ma on a dacite tuff. We obtained a biotite date of 37.43±0.03 Ma on a dacite breccia, possibly equivalent to the dacite tuff. Biotite from the Target Hill rhyolite yielded a K-Ar date of 35.4±1.4 Ma, indistinguishable from, but with a much larger uncertainty, than our sanidine $^{40}Ar/^{39}Ar$ date of 35.97±0.03 Ma.

Three published K-Ar dates are significantly older than any we determined: the 39.0±0.8 Ma date from the Rustler pit, 40.8±1.6 Ma (plagioclase, Richmond Mountain Andesite stratigraphically below our sample H11-107, which has a whole rock isochron date of 35.36±0.24 Ma), and 38.7±1.3 Ma (hornblende, Ratto Spring andesite-dacite

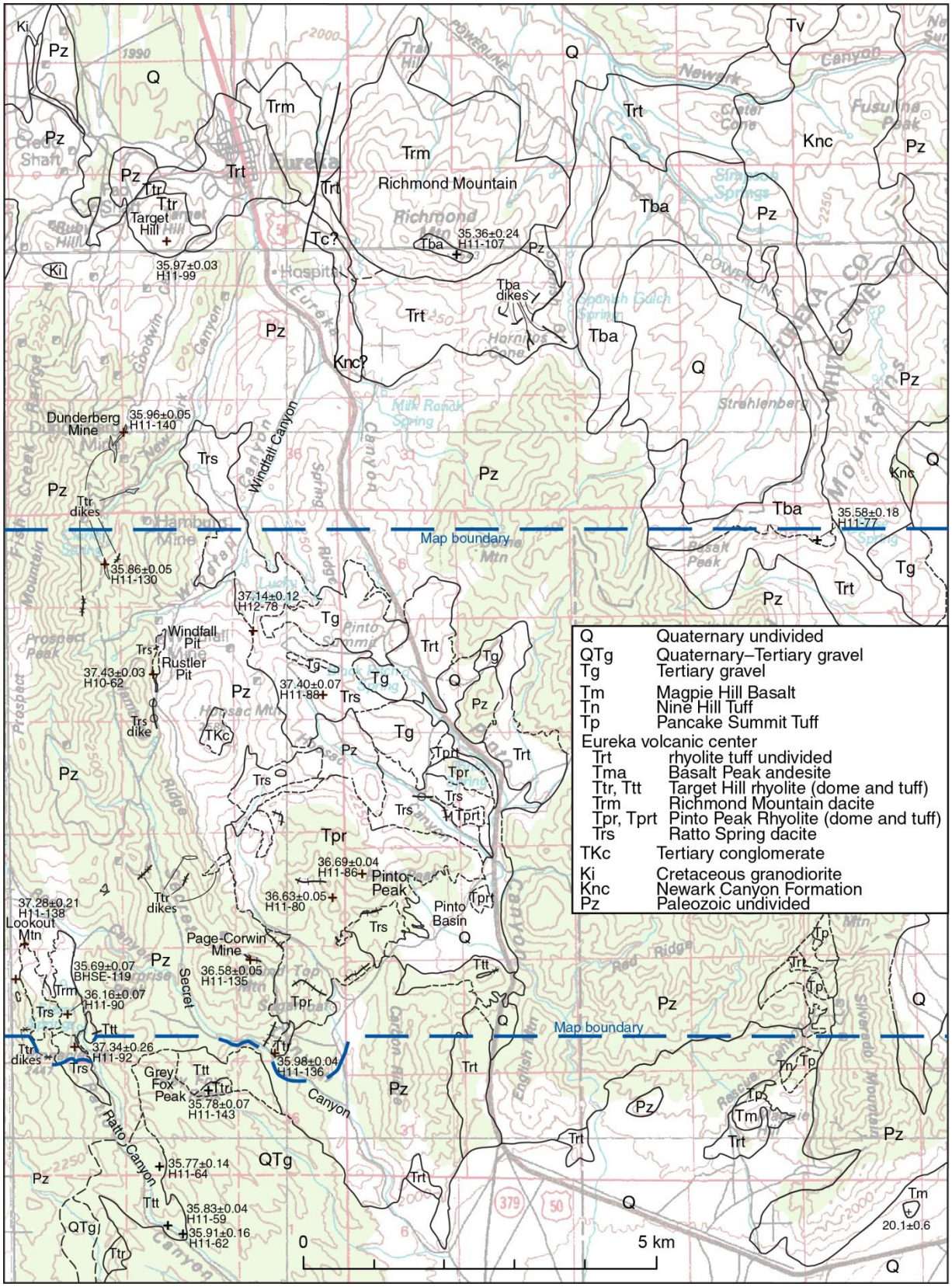

Figure 2. Simplified geologic map of the Eureka volcanic center showing established and revised units of the volcanic center, locations of geographic features discussed in the text, and $^{40}Ar/^{39}Ar$ sample locations and ages.

Table 1. 40Ar/39Ar and U-Pb ages, Eureka volcanic center and other igneous rocks, Nevada.

Sample	Map Unit	rock type	Location	Material	Ages (Ma)[1]										Latitude	Longitude
					wtd mn	± 2σ	n[2]	K/Ca	± 2σ						NAD27	
Single crystal analyses																
H11-59	Ttt	Dacite tuff in quarry	south Ratto Canyon	sanidine	**35.83**	0.04	8/11	16.8	28.0						39.37615	-115.97514
H11-143	Ttr	Rhyolite lava dome	Grey Fox Peak	sanidine	**35.78**	0.07	14/14	75.4	25.6						39.39252	-115.96745
H11-136	Ttr	Rhyolite lava dome	south Ratto Canyon	sanidine	**35.98**	0.04	15/16	50.7	34.4						39.39688	-115.95701
H11-99	Ttr	Target Hill rhyolite lava dome	Target Hill	sanidine	**35.97**	0.03	15/18	62.8	44.0						39.50146	-115.97250
BHSE-119-148'	Ttrd	Rhyolite dike from drill hole	Lookout Mountain	sanidine	**35.69**	0.07	14/14	79.0	18.2						39.39900	-115.99500
H11-130	Ttrd	Rhyolite dike	upper Windfall Canyon	sanidine	**35.86**	0.05	17/17	66.4	59.2						39.46008	-115.98349
H11-140	Ttrd	Rhyolite dike	Dunderberg Mine	sanidine	**35.96**	0.05	14/15	74.8	47.4						39.47732	-115.98065
H11-110	"Ttr"	Rhyolite porphyry	west Garden Pass	sanidine	**36.05**	0.04	14/18	65.7	37.4						39.83704	-116.19997
H11-113	"Ttr"	Rhyolite porphyry	east Garden Pass	sanidine	**35.98**	0.04	17/18	ND							39.82988	-116.19073
H10-114	"Ttr"	Rhyolite ash-flow tuff	Mount Hope	sanidine	**36.03**	0.05	9/9	ND							39.80079	-116.18568
H11-135	Tprd	Rhyolite dike	Page-Corwin area	sanidine	**36.58**	0.05	17/17	ND							39.40971	-115.96022
H11-80	Tprx	vitroclastic band in Pinto Peak complex	Pinto Peak dome	sanidine	**36.63**	0.05	13/15	57.3	51.7						39.41755	-115.94755
H11-86	Tpr	Rhyolite lava dome	top of Pinto Peak	sanidine	**36.69**	0.04	13/15	ND							39.42009	-115.94234
Step heating analyses					plateau	±2σ	%^{39}Ar[3]	steps	isochron	±2σ	^{0}Ar/^{36}Ar	±2σ	total gas	±2s		
H11-107	Trma	Aphyric andesite	Richmond Mountain	matrix	36.16	0.12	47.8	6/8	**35.36**	0.24	423	19	36.69	0.05	39.49920	-115.92598
H11-77	Trma	Aphyric andesite	northeast map area	matrix01	**35.58**	0.18	54.0	3/7	35.48	0.12	294	1	35.55	0.08	39.46217	-115.86688
"	"	"	"	matrix02	**35.67**	0.16	55.2	4/11	36.04	0.14	273	9	35.22	0.06	"	"
H11-62	Ttt	Dacite tuff, top of section	south Ratto Canyon	biotite	**35.91**	0.16	90.6	4/13	35.46	0.08	336	6	35.91	0.04	39.37513	-115.97200
H11-64	Ttt	Dacite tuff, lower part of section	south Ratto Canyon	plagioclase	**35.77**	0.14	100.0	6/6	35.84	0.07	287	25	35.80	0.22	39.38298	-115.97474
H10-106	"Ttr"	Rhyolite porphyry	Mount Hope	K feldspar	**36.04**	0.12	89.4	9/10	35.8	0.4	340	60	34.04	0.20	39.79244	-116.18459
H10-108	"Ttr"	Rhyolite intrusive breccia	Mount Hope	biotite	**36.15**	0.13	95.8	8/11	36.22	0.12	289	10	36.11	0.13	39.79309	-116.18523
H10-114	"Ttr"	Rhyolite ash-flow tuff	Mount Hope	sanidine	**35.92**	0.15	59.4	5/8	NM				35.99	0.09	39.80079	-116.18568
H11-90	Trmv	Plag-Bi-Hbl dacite	Ratto Canyon	plagioclase	**36.16**	0.07	92.0	6/8	36.22	0.05	277	26	36.01	0.14	39.40238	-115.99060
H12-78	Trsv	Dacite volcaniclastic	Windfall Canyon	plagioclase	**37.14**	0.12	100.0	14/14	37.12	0.12	299	6	37.15	0.22	39.45139	-115.95933
H11-88	Trsv	Dacite block and ash-flow tuff	upper Hoosac Canyon	biotite	**37.40**	0.07	89.4	4/12	37.32	0.04	329	10	37.50	0.04	39.44269	-115.94683
H11-92	Trs	Plag-Hbl-Bi low-Si rhyolite lava	Ratto Canyon	hornblende	**37.34**	0.26	94.0	6/10	37.40	0.14	278	31	37.29	0.57	39.39799	-115.98989
H10-62	Trsv	Dacite breccia	Rustler pit	biotite	**37.43**	0.03	62.8	6/10	37.43	0.04	294	5	37.64	0.04	39.44545	-115.97562
H11-138	Trsv	Dacite breccia	Lookout Mountan pit	hornblende	**37.28**	0.21	100.0	7/7	37.31	0.10	287	25	37.27	0.38	39.41140	-115.99837
U-Pb analyses					TuffZirc	+	-	Conc	± 2σ	^{207}Pb/^{206}Pb						
NMC609C-939'	Ki	Cretaceous granite from drill hole	Rocky Canyon	zircon	**87.42**	0.78	0.82	**86.09**	0.84						39.43200	-116.00200
H11-218	Ti?	Igneous rock?	Lookout Mountan pit	zircon	NM			NM		1104 to 2712					39.41592	-116.00093

All ^{40}Ar/^{39}Ar analyses were at the New Mexico Geochronological Research Laboratory (methodology in McIntosh et al., 2003). Neutron flux monitor Fish Canyon Tuff sanidine (FC-1) with assigned age = 28.201 Ma (Kuiper et al., 2008). Sanidine and plagioclase were separated from crushed, sieved samples by standard magnetic and density techniques, leached with dilute HF to remove matrix, and handpicked. Weighted mean ^{40}Ar/^{39}Ar ages of sanidine calculated by the method of Samson and Alexander (1987).

Decay constants after Min et al. (2000); λ_{total} = 5.463 x 10^{-10} yr^{-1}. Isotopic abundances after Steiger and Jäger (1977); ^{40}K/K = 1.167 x 10^{-4}

1 wtd mn = weighted mean. Ages in bold are best estimates of emplacement or deposition age.

2 number of single grains used in age calculation/total number of grains analyzed.

3 %^{39}Ar = percentage of ^{39}Ar used to define plateau age.

All U-Pb analyses were by LA-ICP/MS at the (U-Th)/He Geo- and Thermochronology Lab, The University of Texas at Austin, Daniel Stockli, Director

TuffZirc = weighted mean of ^{206}Pb/^{238}U ages of coherent group of 13 analyses (Ludwig, 2008; Ludwig and Mundil, 2002); Conc = Concordia intercept age of all concordant analyses. ^{207}Pb/^{206}Pb = range of ^{207}Pb/^{206}Pb ages

near our sample H11-90, which has a plagioclase date of 36.16±0.07 Ma) (Blake et al., 1975). We suspect these older dates indicate the larger uncertainty inherent in K-Ar dating. However, the possibility of igneous activity older than we have documented should be considered. K-Ar dates are discussed below where appropriate.

Mortensen et al. (2000) determined U-Pb zircon dates on the Target Hill rhyolite of 35.4±0.2 Ma, slightly younger than our sanidine date of 35.97±0.03 Ma, and on the west Garden Pass stock of 33.1±0.3 Ma, distinctly younger than our sanidine $^{40}Ar/^{39}Ar$ date of 36.05±0.04 Ma, which agrees well with our east Garden Pass (35.98±0.04 Ma) and Mount Hope dates (35.92±0.15–36.15±0.13 Ma). Location descriptions by Mortensen et al. (2000) indicate that their Target Hill sample probably came from within 300 m of our sample and certainly within the same lava dome, and their west Garden Pass stock sample probably was from the same outcrop.

The difference between the Target Hill dates is small and may be explained by slight Pb loss from the analyzed zircons, which Mortensen et al. (2000) discuss. The difference between the west Garden Pass dates is too large to explain easily. Mortensen et al. (2000, p. 434) state that their sample provided "a small amount of poor clarity zircons" with "extremely high U concentrations (14,360–17,530 ppm)". Although their date is the average of two concordant fractions, possibly these zircons had greater Pb loss than recognized.

Ratto Spring Dacite

Cenozoic magmatism began at ~37.4 Ma with eruption of moderately to abundantly and generally coarsely-porphyritic dacite that mostly formed coarse volcaniclastic deposits with some lavas (tables 2, 3; note: ***Table 3:*** *Chemical analyses of igneous rocks of the Eureka volcanic center, Nevada*, is included in a separate file). Phenocrysts are mostly plagioclase, hornblende, biotite, orthopyroxene, ± quartz. Ratto Spring dacite samples mostly contain 69 to 71% SiO_2 and plot in the dacite field; one sample has ~64% SiO_2, and another sample of uncertain affinity has 62% (figs. 3, 4). The most silicic samples plot along the boundary between dacite and rhyolite in the IUGS classification. The rocks are similar to many rocks in northern and eastern Nevada, but less alkalic than those around the Carlin trend (Henry and Ressel, 2000; Ressel and Henry, 2006).

Five $^{40}Ar/^{39}Ar$ dates from the Ratto Spring dacite range from 37.43±0.07 to 37.14±0.12 Ma (table 1). A biotite K-Ar date of 37.7±1.3 Ma on sample PS68-1 (Nolan et al., 1974; Blake et al., 1975) north of our map area and near our chemically analyzed but not dated sample H11-126 supports our assignment of the volcanic rocks in that area to Ratto Spring dacite.

Ratto Spring rocks partly filled deep canyons cut into steeply east-dipping Paleozoic rocks, where resistant units including Hamburg dolomite (Ch) and Eureka Quartzite (Oe) formed ridges and non-resistant units including Secret Canyon Shale (Cs) and Chainman Shale (Mc) formed valleys. Present-day topography largely mimics this paleotopography. Major examples are a narrow, ~1 km wide and possibly 400 m deep paleocanyon in present-day Ratto and Rocky Canyons, immediately east and southeast of Lookout Mountain, and an ~3 km wide and ~400 m deep canyon (or valley) between Hoosac Mountain and Woodpeckers Peak. Preserved deposits in Ratto Canyon range in present-day elevation from 2406 m, where coarse dacite volcaniclastic rocks dated at 37.28±0.21 Ma overlie mineralized rock at the south edge of the Lookout Mountain pit, to 2202 m at the bottom of the canyon. An exploration drill hole by Echo Bay (BR-17) near the canyon bottom encountered another ~200 m of porphyritic dacite to a depth of ~2054 m. Echo Bay interpreted that the volcanic rocks were downdropped by a steeply east-dipping fault, so the contributions of paleorelief versus faulting are uncertain. Preserved deposits range from a maximum elevation of ~2502 m on the east flank of Hoosac Mountain, to 2502 to 2120 m in the lower, eastern part of Hoosac Canyon. However, slight post-volcanic eastward tilting exaggerates the primary relief and thickness of the Ratto Spring dacite in this paleovalley. Depositional contacts of Ratto Spring rocks vary from dipping gently into paleocanyons, e.g., in the Lookout Mountain pit, to steep and near vertical, e.g., in the Rustler and Windfall pits and along the contact with upper conglomerate of the Carbon Ridge Formation (Pcrc) south of Windfall Canyon.

The Ratto Spring rocks probably erupted from multiple sources in the map area including beneath Pinto Peak, along a north-striking fault zone through the Rustler and Windfall pits, and in Ratto Canyon. A source beneath Pinto Peak is indicated by the presence of massive lavas, coarse volcaniclastic deposits, and a dike that crops out on the lowest flanks of Pinto Peak beneath Pinto Peak Rhyolite. Sources in the Rustler-Windfall and Ratto Canyon areas are indicated by particularly coarse volcaniclastic rocks in both areas, a dike in the Rustler pit, and massive lavas in Ratto Canyon.

Pinto Peak Rhyolite

Magmatism resumed in the Eureka area at ~36.6–36.7 Ma with emplacement of the Pinto Peak Rhyolite, the older of two similar rhyolite suites. Nolan et al. (1974) assigned essentially all of the rhyolitic rocks in the Eureka area to this unit, especially assigning all tuffaceous deposits to one of two tuff members. However, three sanidine $^{40}Ar/^{39}Ar$ dates are 36.69±0.04 Ma (H11-86, top of Pinto Peak lava dome), 36.63±0.05 Ma (H11-80, coarse breccia from the interior of the Pinto Peak dome complex), and 36.58±0.05 Ma (H11-135, dike from near the Page-Corwin Mine). In contrast, dates on Target Hill rhyolite from Target Hill and all dates on pyroclastic rocks range between 35.98±0.04 and 35.69±0.07 Ma.

Table 2: Phenocryst data for igneous rocks of the Eureka volcanic center, Nevada.

		Phenocrysts																	
	Map	total %	plagioclase		quartz		sanidine		biotite		hornblende		clinopyroxene		orthopyroxene		garnet	
Map Unit	symbol		%	diam	%	diam	%	diam	%	diam	%	diam	%	diam	%	diam	%	diam
Magpie Hill Basalt	Tmh	0–1	0–1	up to 25														
Nine Hill Tuff	Tnh	2–5	tr	~1	tr	~1	2–5	.3–2	tr	.5								
Pancake Summit Tuff	Tps	40	8		14		16		2		<1							
Basalt Peak andesite	Trma	0–5	0–4	.2–4									0–.5	.2	0–1	.2		
Target Hill rhyolite	Ttr	15-20	2–4	.1–1.5	5–10	.5–2.5	7–10	.1–2.5	.5–2.5	.1–1.5	0–tr	.1–.2			0–.5	.1–.3	?	
lava flow	Ttrf	5	4	.1–1.5					1	.1–1								
dacite ash-flow tuffs	Ttt	40	25–30	.1–2.5	0–3	.5–3	tr	.2–1.5	1–3	.1–2	2–6	.05–1.5	0–3	.1–.5	0–5	1–.8		
rhyolite ash-flow tuff		25	2	.2–1.5	10	.5–2.5	10	.1–2	1	.1–.8								
Richmond Mountain dacite	Trmv	35	25	.3–3(8)	0–tr	2			4.5	.2–4	2.5	.1–2	tr	<1	.5	<1		
Pinto Peak Rhyolite	Tpr, Tprx, Tprf, Tprd, Tprt	15–25	5–8	.1–2.5	4–10	.4–8	4–10	.2–10	.5–1.5	.1–2							0–.5	.1–.8
Ratto Springs dacite	Trs, Trsv, Trsd	25–35	15–25	.2–3	0–3	.5–3			0–3	.1–2	3–5	.1–2	0?		0–2	.1–1		

% = volume percent; diam = diameter in millimeters; tr = trace

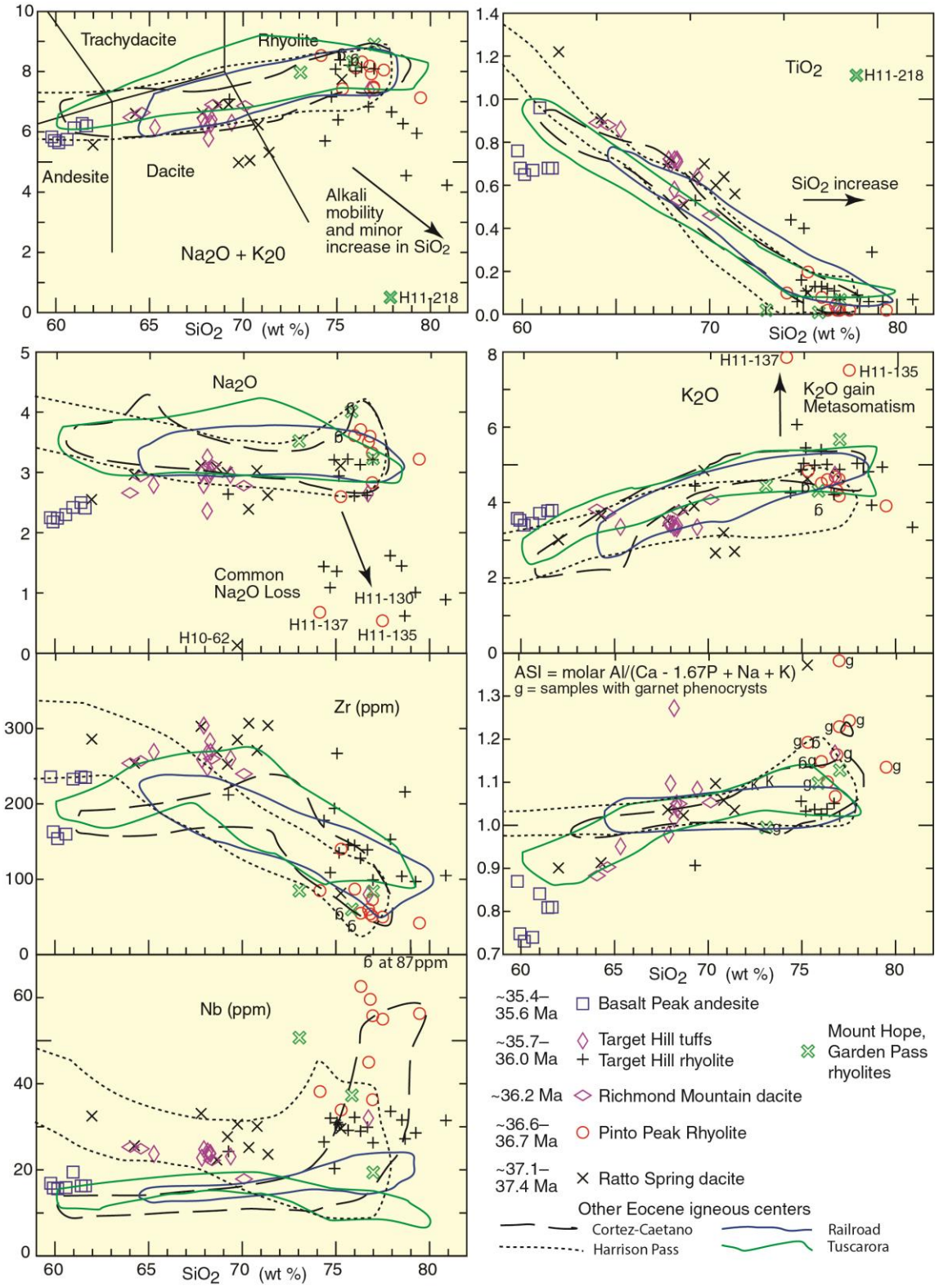

Figure 3. Plots showing compositional characteristics of igneous rocks of the Eureka volcanic center (EVC), Mount Hope and Garden Pass, and fields for several other Eocene igneous centers. EVC rocks are similar to but less alkalic and more aluminous than contemporaneous rocks of these other centers (Henry and Ressel, 2000; Ressel and Henry, 2006). EVC rocks are mostly unaltered but a few have undergone minor alkali mobility. The text discusses the significance of the alteration for timing of Carlin-type mineralization.

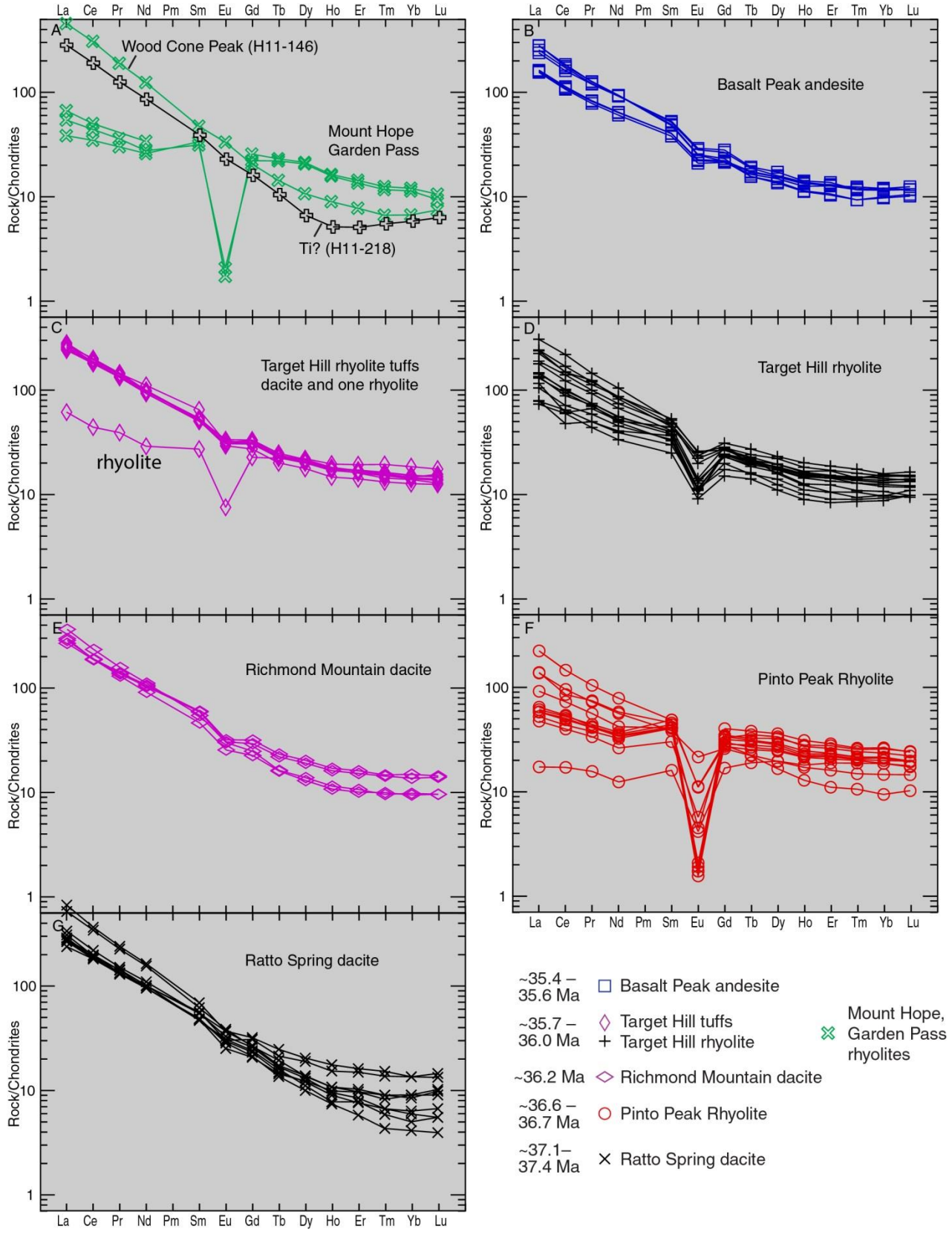

Figure 4. Chondrite-normalized rare-earth element (REE) plots of igneous rocks of the Eureka volcanic center and a few regional units. Rhyolites of the Pinto Peak Rhyolite are more evolved (lower LREE, higher HREE) than are Target Hill rhyolites.

Distinguishing Pinto Peak and Target Hill rhyolite other than by age is equivocal. Both sequences are moderately porphyritic, and phenocrysts are mostly sanidine and commonly bipyramidal quartz, with generally lesser plagioclase and biotite. Pinto Peak Rhyolites generally are more coarsely porphyritic, with sanidine and quartz phenocrysts up to 10 mm in diameter, commonly contain garnet phenocrysts, lack hornblende phenocrysts, and are slightly more chemically evolved, with higher Rb, Y, Nb, Ta, HREE, and aluminum saturation indices (consistent with the common presence of garnet) and lower TiO_2, FeO, Sr, Zr, Hf, and LREE (figs. 3, 4). However, none of these characteristics may be diagnostic, because dike sample BHSE-119-148 (drill hole cuttings) dated as part of the Target Hill rhyolite is compositionally similar to nearby coarsely-porphyritic rhyolites, and rhyolites of Target Hill age at Garden Pass ~40 km northwest of Eureka also contain garnet. Distinguishing pyroclastic deposits is particularly difficult. All dated pyroclastic rocks have Target Hill ages, so only those deposits that are close to Pinto Peak and clearly underlie Pinto Peak dome rock are assigned to the Pinto Peak Rhyolite.

The Pinto Peak Rhyolite consists mostly of the 3-km-diameter, semi-coalesced lava dome that is roughly centered on Pinto Peak (fig. 2). The dome consists of a complex mix of massive rhyolite, coarse breccia, and coarse to fine pyroclastic deposits, all cut by several rhyolite dikes. Steep contacts with surrounding coarse marginal breccia and pyroclastic deposits and generally steep, concentric flow bands indicate the rhyolite probably extruded in a roughly cone shape through surrounding breccia and tuff (Tprx, Tprt) to form a series of semi-coalesced lava domes. Breccia was probably largely derived from collapse off the flank of the rising lava dome. It is likely that none of the rocks in the lava dome flowed significant lateral distances. The lava dome near Pinto Spring is mapped as Pinto Peak Rhyolite because it is stratigraphically low, cuts or overlies Ratto Spring deposits, and is close to Pinto Peak. The lava dome that includes Sugarloaf in Dale Canyon is mapped as Pinto Peak Rhyolite because a coarse, garnet-bearing dike (H11-82) cuts it.

The most distal dated Pinto Peak Rhyolite is the dike near the Page-Corwin Mine, which is only ~600 m from the southwestern edge of the dome complex (fig. 2). All dated domes, dikes, and pyroclastic deposits farther away give Target Hill rhyolite ages. The Pinto Peak Rhyolite may be restricted to the immediate vicinity of Pinto Peak.

Garnet-bearing rhyolites are present in three nearby areas (fig. 1): Garden Pass, which is ~40 km northwest of the map area and discussed with the Target Hill rhyolite; in the northern Sulphur Spring Range about 75 km to the north; and near Ely about 90 km to the east. A dacite to rhyolite tuff with phenocrysts of plagioclase, biotite, quartz, and Fe-rich garnet (~82% almandine – 18% pyrope – ≤1% spessartine) and with a U-Pb zircon date of 35.5±0.4 Ma is widespread in the northern Sulphur Spring Range (Ryskamp et al., 2008). Andesite lavas that are ~31.4 Ma have resorbed garnets (74-86% almandine – 20-12% spessartine – ≤6% pyrope) that Ryskamp et al. (2008) interpreted to be xenocrysts resulting from mixing of silicic and mafic magmas. The source of the dacite tuff is unknown and conceivably in the Eureka area.

The 36.7 Ma rhyolite of Garnet Hill near Ely (fig. 1) has lithophysal (intense, post-magmatic, vapor-phase) almandine-spessartine garnet in vugs (Pabst, 1938; Brokaw et al., 1973; Hollabaugh and Purcell, 1987; Gans et al., 2001), and not as phenocrysts as in the rocks at Eureka or the Sulphur Spring Range. However, the Garnet Hill rhyolite is apparently also strongly peraluminous, and indistinguishably the same age as Eureka garnet-bearing rocks. The Garnet Hill garnets are 69.3% almandine–28.5% spessartine (Pabst, 1938).

Richmond Mountain Dacite

The Richmond Mountain dacite is petrographically and compositionally similar to Ratto Spring dacite, although only four samples have chemical analyses (table 2; figs. 3, 4). The Richmond Mountain Andesite of Nolan et al. (1971) combined the abundantly porphyritic dacites of our Richmond Mountain dacite with aphyric to very sparsely porphyritic andesites, which are what we call Basalt Peak andesite. We separate them into the two units because field relationships and dating demonstrate that they are temporally distinct, and they are petrographically and compositionally distinct. The porphyritic rocks are all dacite, and the aphyric rocks are all andesite.

The abundantly porphyritic rocks contain phenocrysts mostly of plagioclase, with biotite, hornblende, and orthopyroxene, and a few samples contain traces of quartz or clinopyroxene (table 2). Four chemical analyses of Richmond Mountain dacite vary from 64 to 70% SiO_2 and largely overlap with Ratto Spring dacite (figs. 3, 4).

The Richmond Mountain dacite crops out in our map area only in Rocky Canyon and upper Ratto Canyon where they consist of coarse volcaniclastic deposits. These deposits crop out almost to the bottom of the canyon, at the same or lower elevation than some Ratto Spring dacite, which shows that the Ratto Spring dacite was deeply eroded before deposition of Richmond Mountain dacite. The coarseness of the deposits indicates a nearby but unidentified source.

Richmond Mountain dacite at and around Richmond Mountain, north of the map area, includes coarse lava flows. The mountain itself is a slightly northeast-inclined lava dome of hornblende dacite. Flow bands in the dacite dip steeply inward, especially around the steep southwestern side where the dacite is as much as 200 m thick. Richmond Mountain probably was a major source for the unit.

We determined only one $^{40}Ar/^{39}Ar$ date, 36.16±0.07 Ma, on plagioclase from sample H11-90 in Ratto Canyon (table 1). Blake et al. (1975) report K-Ar dates of 36.5±1.3 Ma on hornblende from sample PS88-6 from the southwest

flank of the Richmond Mountain lava dome and 40.8±1.6 Ma on plagioclase from sample HG434, probably topographically below PS88-6. The first K-Ar date agrees well with our date, but the second is much older and the oldest reported date on Eureka Cenozoic rocks. Blake et al. (1975) report no information about rock type or analytical data for this sample, and its location is unclear.

Target Hill Rhyolite

Target Hill rhyolite is the younger of two similar rhyolite suites that consist of lava domes, coarse marginal breccias around domes, apparently the most voluminous part of the pyroclastic-flow, -fall, and -surge deposits of the Eureka area, and dikes. Initially named rhyolite of Target Hill (Nolan et al., 1971) for Target Hill next to Eureka ~4 km north of the map area boundary, Nolan et al. (1974) and Blake et al. (1975) assigned these rocks to the formal Pinto Peak Rhyolite. Precise $^{40}Ar/^{39}Ar$ dating shows that Target Hill rhyolites intruded at ~35.9 Ma and are distinctly younger than Pinto Peak Rhyolites, which are ~ 36.6 Ma. Target Hill rhyolites contain 15 to 20% phenocrysts of quartz and sanidine, lesser plagioclase, minor biotite, and in less silicic samples, a trace of hornblende and/or orthopyroxene (table 2). This assemblage is similar to that of Pinto Peak Rhyolites but is mostly more finely porphyritic, with phenocrysts all ≤2.5 mm. Also, garnet has not been found in any Target Hill rocks in the map area or near Target Hill. Chemical analyses show that rhyolites of the Target Hill unit are slightly less evolved than Pinto Peak Rhyolites, with higher TiO_2, FeO, Sr, Zr, Hf, and LREE and lower Rb, Y, Nb, Ta, HREE, and aluminum saturation indices (figs. 3, 4); the lower saturation index is consistent with the absence of garnet.

The Target Hill rhyolite is much more widespread than the Pinto Peak Rhyolite (fig. 2). The largest single lava dome is Target Hill itself, but many dikes and small lava domes occur from Target Hill to south of our map area. Several dikes from the Dunderberg Mine south to the headwaters of Windfall Canyon are part of Target Hill rhyolite based on sanidine $^{40}Ar/^{39}Ar$ dates on two samples (35.96±0.05 Ma, H11-140, Dunderberg Mine; 35.86±0.05 Ma, H11-130, New York Canyon), similar fine phenocryst assemblage, and similar chemical composition. Target Hill rhyolite also includes the small lava dome at Grey Fox Peak (35.78±0.07 Ma, H11-143) and the underlying pyroclastic sequence in lower Ratto Canyon.

Another group of dikes exposed from south of Lookout Mountain to Hamburg Ridge west of Pinto Peak and the lava dome that cuts the Sugarloaf part of Pinto Peak Rhyolite are Target Hill rhyolite based on two sanidine $^{40}Ar/^{39}Ar$ dates (35.98±0.04 Ma, H11-136, lava dome; 35.69±0.07 Ma, BHSE-119-148, dike from drill hole south of Lookout Mountain) and similar composition, especially high TiO_2, which indicates all are dacites and relatively unevolved rhyolites. However, this group of dikes is coarsely porphyritic, unlike most Target Hill rhyolite. The younger date may indicate that Target Hill rhyolite magmatism was relatively prolonged.

The inset map area of pyroclastic rocks in the southern part of Ratto Canyon, south of the main map area, was mapped because it had the thickest, best-exposed section of tuffaceous rocks in the Eureka area. Based on age, all are Target Hill rhyolite. In ascending stratigraphic order, $^{40}Ar/^{39}Ar$ dates are 35.77±0.14 Ma, plagioclase, H11-64; 35.83±0.04 Ma, sanidine, H11-59; 35.91±0.16 Ma, biotite, all on dacite tuffs. The more precise sanidine date provides the best age estimate. Rhyolites dominate the lower part of the section but were not sampled for chemical analysis because outcrops were generally weathered. Dacite ash-flow tuffs with a few interbedded rhyolites dominate the upper part. The dacites are compositionally similar to the high-TiO_2 group of dikes south of Lookout Mountain and may be derived from them.

The intrusive rhyolite complex at Mount Hope, which hosts a giant porphyry Mo deposit (Westra and Riedell, 1996), and the west and east Garden Pass rhyolite stocks ~40 km northwest of Eureka (fig. 1) are the same age as the Target Hill rhyolites (table 1) but have some petrographic and compositional characteristics of Pinto Peak Rhyolites. Most notably, the Garden Pass rhyolites contain garnet phenocrysts, and both Garden Pass and Mount Hope rocks are as highly evolved as Pinto Peak Rhyolites, with mostly high Rb, Nb, and Ta, low TiO_2, Sr, Zr, and LREE, and large Eu anomalies (table 3; figs. 3, 4; Westra and Riedell, 1996). However, the Mount Hope–Garden Pass rocks do not have the high Y or HREE that is characteristic of Pinto Peak Rhyolites. Mount Hope consists of complexly, shallowly inter-intruded rhyolites (quartz porphyrys), breccias, and accompanying rhyolitic tuffs (Westra and Riedell, 1996). The Mount Hope Mo deposit contains 1.3 billion pounds of Mo in proven and probable reserves and is currently in development (General Moly, Inc.; www.generalmoly.com/). The Garden Pass intrusions are partly cross-cutting, partly sill-like bodies that intrude upper-plate Ordovician Vinini Formation. Westra and Riedell (1996) report that garnets in the Garden Pass intrusions are almandine-spessartine, ranging from 64.7% almandine–25.2% spessartine, similar to Garnet Hill garnets, to 47.8% almandine–50.5% spessartine.

Basalt Peak Andesite

The Basalt Peak andesite consists of aphryic to very sparsely porphyritic, andesite lava flows and shallow intrusions that crop out from the northeastern edge of our map area, the location of Basalt Peak, northwestward to and slightly beyond Richmond Mountain (fig. 2). It constitutes the aphyric, andesitic part of the Richmond Mountain Andesite of Nolan et al. (1971) and Blake et al. (1975). Phenocrysts are mostly plagioclase, either as 0.2 mm microphenocrysts or larger, highly resorbed grains to

4 mm, along with fine ortho- and clinopyroxene (table 2). The rock is relatively homogeneous with 60 to 62% SiO_2 (figs. 3, 4). The analyzed samples show two groups based on small differences in trace elements, especially Zr and REE. The two flows from the northeastern part of the map area and a dike (H11-102) from south of Richmond Mountain have lower Zr and LREE and higher HREE (i.e., shallower REE slopes) than the flows that cap Richmond Mountain and a strongly columnar-jointed, irregularly elliptical intrusion (H11-103) north of sample H11-102.

The Basalt Peak andesite was deposited on an irregular surface cut into various older rocks, including Richmond Mountain dacite on Richmond Mountain, undivided pyroclastic rocks in the northeastern part of the map area and around Richmond Mountain, and on Paleozoic rocks between Richmond Mountain and the map area. This variation attests to the continued rapid erosion of volcanic rocks and maintenance of major pre-volcanic topography during volcanism. Rocks mapped as Basalt Peak andesite (originally Richmond Mountain Andesite) just northwest of Pinto Summit (Nolan et al., 1974) are all coarse gravel composed mostly of the aphyric andesite clasts (Tcrm). Sources probably include Basalt Peak and dikes south of Richmond Mountain (fig. 2).

At 35.4–35.6 Ma, the Basalt Peak andesite is the youngest igneous rock of the Eureka volcanic center. $^{40}Ar/^{39}Ar$ dates of two splits of matrix from a flow (H11-77) from the northeast part of the map area are 35.58±0.18 and 35.67±0.16 Ma (table 1). The flow capping Richmond Mountain has a slightly disturbed spectrum that yields a good isochron date of 35.36±0.24 Ma.

Igneous(?) Rock of Unknown Age: Possible Dike, Lookout Mountain Pit

A possible dike (Ti) was mapped in and north of the Lookout Mountain pit, but chemical analysis and U-Pb zircon dating indicate that the rock in the pit is probably not an igneous rock. The "dike" is an irregular, dike- or sill-shaped body that cuts Hamburg dolomite in the pit and Lone Mountain Dolomite farther north. The rock is strongly bleached white in the pit and tan or light brown to the north, where it is as much as 10 m thick. Rock in the pit has common jasperoid fragments (Tj), which are interpreted to have been altered in the Cenozoic. Sample H11-218 of highly altered "dike" from the Lookout Mountain pit consists of very fine-grained (≤10 micrometer) quartz, clay, and opaques and is almost all SiO_2 (77.9%), Al_2O_3 (18.9%), FeO (1.30%), and TiO_2 (1.11%) (table 3). The silica content suggests a rhyolite, but the high TiO_2 indicates a much more mafic rock and is higher than all but one analyzed igneous rock in this study (fig. 3). The rock has an unusual REE pattern, a steep negative slope that turns slightly positive in the HREE, but is somewhat similar to those of the Ratto Spring dacite and of the quartz monzonite of Wood Cone Peak (fig. 4), a 34.1±1.5 Ma (biotite K-Ar; Marvin and Cole, 1978) intrusion ~4.4 km southwest of the southwest corner of our map area (fig. 1). Sample H11-218 yielded only about 15 zircon grains, all except two of which are well rounded, oval, and less than 50 micrometers in longest dimension and give Proterozoic dates ($^{207}Pb/^{206}Pb$ date between 1100 and 1800 Ma; one date = 2700 Ma), all of which indicates the zircons are derived from the host Paleozoic sedimentary rocks. Two zircons are euhedral, more typical of igneous rocks, and give $^{206}Pb/^{238}U$ dates of about 97 Ma. The most likely explanation of all the data is that the rock in the pit is decalcified host rock, the chemical analysis gives the composition of insoluble residue, presumably detrital material in the Hamburg dolomite, and the two euhedral zircons are contamination from sample processing. The rock could be an intensely altered breccia dike or fault gouge. Alternatively, the rock could be a Cretaceous dike that picked up considerable host rock, which dikes commonly do. Cretaceous intrusions with U-Pb zircon dates of 106 Ma are common in the northern part of the Eureka district (Mortensen et al., 2000; Vikre, 1998; Nolan et al., 1971), and a Cretaceous intrusion was encountered in drill hole NMC-609, ~2 km north of the Lookout Mountain pit. Two samples of that body are chemically unlike the pit sample with ~73% SiO_2 and 0.12 and 0.16% TiO_2. Similarly, two analyses of the Ruby Hill granodiorite from the northern part of the district are unlike the pit sample with 62% and 0.45% and 65% and 0.62% SiO_2 and TiO_2, respectively (Vikre, 1998). Sample NMC-609C-939' yielded abundant, large, euhedral zircons that give a TuffZirc (Ludwig, 2008; Ludwig and Mundil, 2002) $^{206}Pb/^{238}U$ date of 87.42+0.78/-0.82 Ma and concordia intercept date of 86.04±0.84 Ma (table 1). Proterozoic dates were found only in two zircon cores. Analyzed Cretaceous intrusions at Eureka have neither the chemical composition nor the possible "age" of sample H11-218. For the pit rock to be a Cretaceous intrusion, alteration would have to have drastically changed its chemical and petrographic characteristics, removing any indication of a formerly coarse-grained granitic rock. These results do not address the age or origin of unit Ti mapped north of the pit, which has not been analyzed or dated.

Comparison of the Eureka Volcanic Center to Other Eocene Igneous Centers

The Eureka volcanic center is part of a major episode of magmatism that migrated south and southwestward across Nevada during the Cenozoic. This magmatism is commonly attributed to rollback, i.e., steepening, of a formerly shallow subducted slab that had flattened beneath western North America beginning in the Late Cretaceous. As the slab rolled back, asthenosphere welled up to replace it and heated the lithosphere, generating magma (Humphreys, 1995; Henry and John, 2013). Cenozoic magmatism began about 47 Ma in northern and northeastern Nevada, migrated across the region,

eventually to form the ancestral Cascade arc in western Nevada and most recently merging imperceptibly into the modern Cascade arc (Cousens et al., 2008). Plots of the initiation of Cenozoic magmatism show a regular south-southwestward progression (Henry and John, 2013); this progression was the initial evidence that led to the rollback interpretation. The contours of initial magmatism show activity beginning at Eureka at ~38 Ma, which is the case. However, because the age contours are partly based on the timing of activity at Eureka, the evidence is somewhat circular.

The Eureka volcanic center is one of many igneous centers that were active in the Eocene across northern Nevada. Because several such centers, including Eureka, are spatially and possibly genetically associated with major mineral deposits, including Carlin-type gold deposits (Cline et al., 2005; Ressel and Henry, 2006; Muntean et al., 2011), and also because Eureka is distinctive in having garnet-bearing rhyolites, the Eureka volcanic center is particularly significant. Eureka is similar in age (~40–35 Ma), overall rock type (dominantly intermediate to silicic intrusive and volcanic rocks and absence of high-volume, rhyolitic, caldera-forming tuffs), extended duration of igneous activity (~2 Ma versus 4 Ma in the Carlin trend and 6 Ma around Cortez), geo-tectonic setting (rollback magmatism), and crustal basement province (in Precambrian basement or similar basement rifted in the late Proterozoic) (Tosdal et al., 2000; Ressel and Henry, 2006; John et al., 2008, 2009; Henry and John, 2013).

Eureka is variably distinctive in two ways: 1) Volcanism was ongoing throughout the time of igneous activity, whereas volcanic rocks were late to absent in other centers. For example, magmatism around the Carlin trend occurred between ~40 and 36 Ma, consisted entirely of abundant dikes interpreted to be offshoots of plutons at depths of 6-10 km between 40 and 38 Ma, and volcanism only began ~38 Ma in the Emigrant Pass volcanic field along the southwest edge of the trend (Ressel and Henry, 2006). Magmatism in the Cortez area occurred between ~40 and 34 Ma and consisted of many intermediate to silicic dikes accompanied by a small volume of extrusive rocks until eruption of the voluminous, caldera-forming Caetano Tuff at 34 Ma (Colgan et al., 2011). All rhyolitic rocks require large-volume plutons to generate silicic magma and dikes, so major plutons underlie all these fields, and igneous activity was fundamentally the same in all areas; and 2) The Eureka volcanic center is distinctive compared to other centers spatially-associated with gold deposits because it includes garnet-bearing, strongly peraluminous rhyolites. Only the 36–37 Ma Harrison Pass pluton in the Ruby Mountains has garnet-bearing and other strongly peraluminous rocks, including two-mica granites (Barnes et al., 2001; Colgan et al., 2010), and the Harrison Pass pluton is not associated with mineralization. Late Cretaceous two-mica granites are also present in our map area (Rocky Canyon and McCullough Butte), the Ruby Mountains, and probably throughout eastern Nevada (Barton, 1987).

Geochemical classification diagrams illustrate the similarity and some differences between the Eureka volcanic center and other Eocene igneous centers in Nevada (figs. 3 and 5), including the 40–39 Ma Tuscarora volcanic field (the oldest and northernmost of the major Eocene centers), the 37–36 Ma, composite Harrison Pass pluton, the 38 Ma Railroad center, and the 35.8 Ma Cortez rhyolites and 34 Ma Caetano Tuff at and near Cortez Hills. Because alkali mobility, especially loss of Na_2O, during weathering or alteration, skews major oxide concentrations, all analyses that appear to have lost Na_2O were omitted. All centers are calc-alkalic, although Eureka is slightly less alkalic on the total alkalis–SiO_2 diagram and classification, has distinctly lower Na_2O, and trends towards calcic according to MALI (modified alkali-lime index; Frost et al., 2001). Eureka samples that have lost Na_2O plot significantly away from the main trends. Eureka rocks are indistinguishable from the other groups in most major oxides.

All Eocene centers contain evolved, high-SiO_2 rhyolites, but these rocks are variably enriched in incompatible trace elements, those not incorporated into phenocrysts, and have variable aluminum-saturation indices (ASI), which measure how peraluminous a rock is (figs. 3 and 5). The most evolved rocks at Eureka, in the Harrison Pass pluton, and in the Caetano Tuff are highly-enriched in Nb, Y, and HREE. The garnet-bearing Pinto Peak Rhyolites have ASI as high as 1.38. Harrison Pass rocks have ASI up to 1.20 and contain garnet or even muscovite along with biotite. The Caetano Tuff has ASI up to 1.16 but lacks either garnet or muscovite. The highest SiO_2 rocks in the Tuscarora volcanic field have ASI similar to the Caetano Tuff, lack garnet, and are not enriched in any of the incompatible trace elements.

The Eureka volcanic center shows two separate trends on several geochemical plots of incompatible elements that relate to peraluminous compositions (fig. 5). Ratto Canyon dacites have lower Y and Yb and higher La/Yb (representative of the ratio of LREE to HREE) than do Richmond Mountain dacites and Basalt Peak andesites with similar SiO_2 (fig. 5). Because garnet incorporates Y and the HREE, these characteristics suggest that the initial Ratto Canyon dacite magmas formed by partial melting of rocks that contained garnet and so retained these elements. The garnet-bearing Pinto Peak Rhyolites contain the highest concentrations of Y and HREE and have the lowest La/Yb among Eureka rocks, as do the most differentiated Harrison Pass and Caetano rocks (fig. 5). It is unclear whether this reflects crystallization of garnet that has incorporated Y and HREE or simply extreme differentiation, because Caetano rocks lack garnet.

Geochemical-tectonic diagrams using the same and additional elements exemplify these differences (fig. 5). The less silicic rocks, except Ratto Canyon dacite, of all centers plot in the volcanic-arc granite field on Yb/Ta and Y+Nb/Rb (Pearce and Peate, 1995) and I&S-type (igneous and sedimentary source) granite field on Ga-

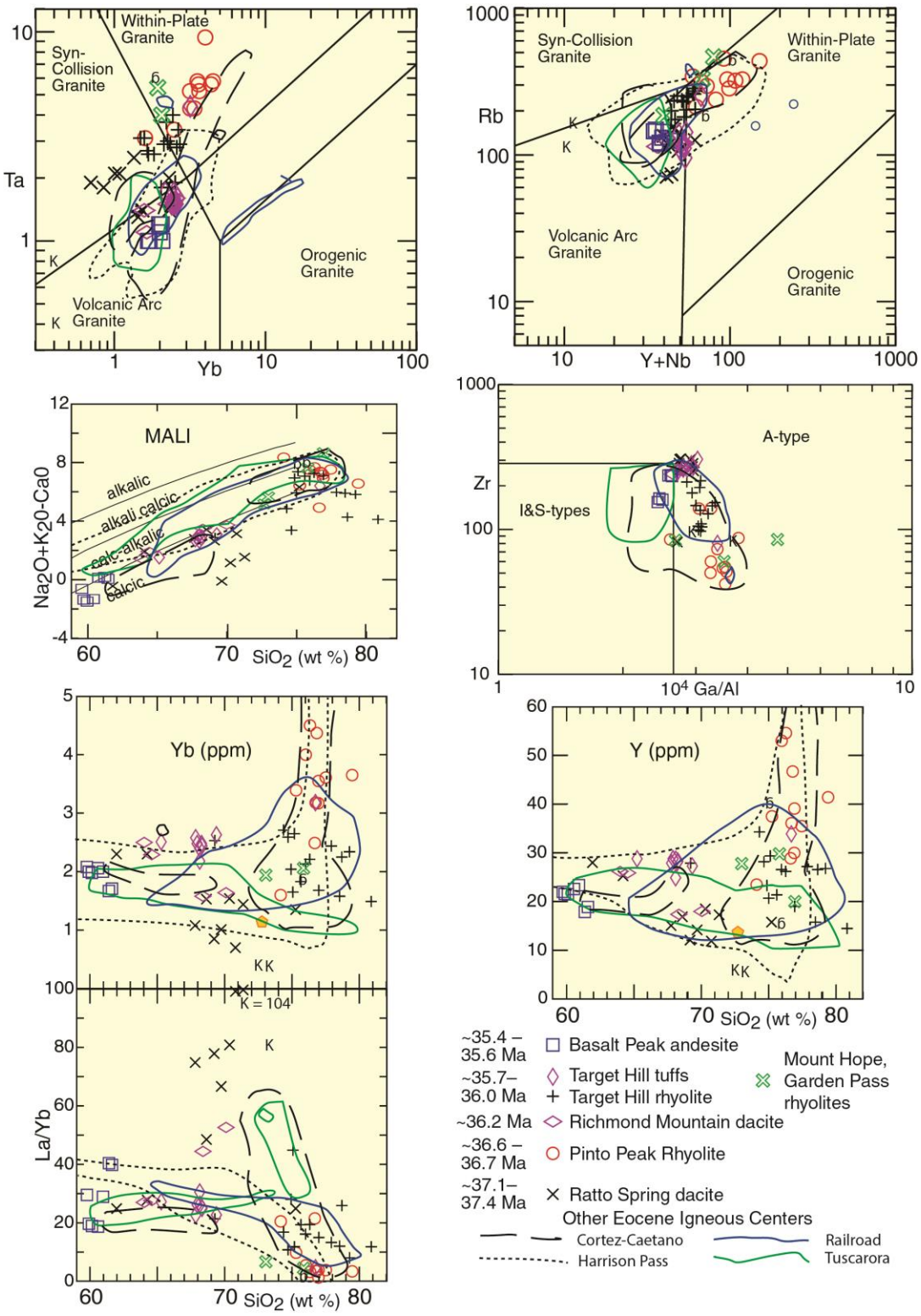

Figure 5. Plots showing additional compositional characteristics of igneous rocks of the Eureka volcanic center and comparison with other Eocene igneous centers. Major- and trace-element discrimination diagrams (Frost et al., 2001; Pearce and Peate, 1995; Whalen et al., 1987) show that most Eocene igneous rocks are calc-alkaline and plot in the volcanic arc granite field. Eureka rocks are more calcic, and Ratto Spring rocks plot in the syn-collision granite field. More evolved compositions trend into within-plate granites and have high contents of incompatible trace elements. See text for detailed discussion.

Al/Zr diagrams (Whalen et al., 1987). This is consistent with their origin related to rollback of the shallow subducted slab. Differentiation drives compositions toward and, for the most differentiated rocks, into the within-plate granite field and A-type (anorogenic or within-plate) granite field. The Ratto Canyon dacites form a separate trend on the Yb/Ta plot, falling in the syn-collision granite field, reflecting their low Yb and high Ta contents. These plots indicate only that differentiation enriches residual magma in these incompatible elements, not to a change in tectonic setting. All these diagrams further suggest that the Ratto Canyon dacites, the Target Hill rhyolite domes and dikes, and the Pinto Peak Rhyolites are a possibly genetically related group, and that the Target Hill rhyolite tuffs and Basalt Peak andesite are a separate, probably unrelated group.

Strongly peraluminous magmas in general, and the most peraluminous parts of the Harrison Pass pluton in particular, are interpreted to have a substantial component of crustal melt, especially of melts of pelitic or metapelitic sedimentary rocks (Kistler et al., 1981; Barnes et al., 2001; Frost et al., 2001). For example, Ryskamp et al. (2008) suggested that the peraluminous, garnet-bearing rocks in the northern Sulphur Springs Range near Eureka resulted from partial melting of pelitic metasedimentary rocks in the thickened crust of eastern Nevada. However, Miller (1985) showed that partial melting of a much wider range of crustal rocks can give rise to peraluminous magmas and that melting of only pelitic rocks generates magmas that are more strongly peraluminous than those at Eureka.

Some tentative conclusions based on all these data are that magmas of the Ratto Canyon dacite have a much greater crustal melt, possibly pelitic, component than do those of the Basalt Peak andesite or tuffs of the Target Mountain rhyolite. Magmas of the Pinto Peak and Target Hill rhyolites could have formed from differentiation of Ratto Canyon dacite or similar magmas. These possibilities can be tested with isotopic and other geochemical analyses. Finally, if magmas are the source of metals and fluids for Carlin-type gold and other mineral deposits (Muntean et al., 2011), the potential involvement of different crustal components in different magma series, even in a single location, suggests that some magmas may be more favorable than others.

NOTE ON PREVIOUS MAPPING OF CRETACEOUS CONGLOMERATE

Within the map area, Nolan et al. (1974) mapped several isolated exposures of conglomerate and other lithologies that lie unconformably over rocks between Ordovician and Permian in age as the Early Cretaceous Newark Canyon Formation. We have re-examined all of these exposures, and we map them as a variety of different rock units, including Permian conglomerate, Late Cretaceous to late Eocene conglomerate, sedimentary rocks associated with late Eocene volcanism, and Quaternary colluvium. Areas of key importance include: 1) the axis of the Sentinel Mountain syncline, where we map unconsolidated and locally-cemented angular limestone cobbles and boulders that lie on Devonian rocks as Quaternary colluvium (Qc); 2) areas in the footwall of the Pinto Summit fault where we map pebble conglomerate with a white, tuffaceous matrix that lies on Silurian rocks as conglomerate associated spatially and temporally with late Eocene volcanism (unit Tcl); and 3) on Hoosac Mountain, where red-matrix, limestone-clast pebble conglomerate that lies on Ordovician rocks in the footwall of the Hoosac fault system, and on Mississippian and Permian rocks in its hanging wall, yields a Late Cretaceous (~72 Ma) youngest detrital zircon population (Long et al., 2014), and is therefore a distinctly younger rock unit (unit KTc) than the Newark Canyon Formation.

Red-matrix, limestone-clast, pebble conglomerate that we map as Newark Canyon Formation is only preserved in the northeast corner of the map area, in a series of exposures that unconformably overlie the Mississippian Diamond Peak Formation and Pennsylvanian Ely Limestone. These exposures form the southern end of a semi-continuous, ~5 km-long exposure that contains the type-section of the Newark Canyon Formation (fig. 1), which has been dated by U-Pb geochronology as Aptian (ca. 116 Ma; Druschke et al., 2010), and unconformably overlies Mississippian, Pennsylvanian, and Permian rocks (Nolan et al., 1971; 1974).

However, north of our map area, near the town of Eureka (fig. 1), Nolan et al. (1971) also mapped conglomerate that unconformably overlies units between Ordovician and Permian in age as the Newark Canyon Formation, and we have not been able to examine all of these outcrops. Without further mapping and age control, it is difficult to definitively assign an age to these rocks, and we suggest that they could range from Early Cretaceous, latest Cretaceous to late Eocene (equivalent to our unit KTc, or to the Elko Formation further to the north), or possibly late Eocene, associated temporally and spatially with volcanism. In particular, the conglomerate that we map on Hoosac Mountain (KTc), which has a similar red-matrix lithology but is distinctly younger than the Newark Canyon Formation, makes correct age assignment difficult without accompanying geochronology or biostratigraphy.

NOTE ON PREVIOUS INTERPRETATIONS OF STRUCTURES

The map area has experienced a multiphase tectonic history of contractional deformation overprinted by extensional deformation. Not surprisingly, interpretations of the style and geometry of several large-offset faults in the map area have varied widely in previous studies (e.g., Nolan et al., 1971; 1974; Taylor et al., 1993; Carpenter et al., 1993; Ransom and Hanson, 1933; Lisenbee, 2001), which has resulted in disagreement over deformation geometry.

One important structure that has had varying interpretations is the Hoosac fault, which has been interpreted as a steeply east-dipping normal fault (Hague, 1892; Nolan et al., 1974; Long et al., 2014) and a shallowly west-dipping thrust fault (Nolan, 1962; Taylor et al., 1993; Lisenbee, 2001). Our mapping reveals that this is not one structure, but a series of anastomosing, steeply east-dipping to subvertical, down-to-the-east normal faults, which we name the Hoosac fault system. The easternmost, master fault of the system, which corresponds to the Hoosac fault defined in previous studies, places Mississippian and Permian rocks over Ordovician rocks, corresponding to omission of ~2–3 km of stratigraphy. To the west of the master fault, a series of subsidiary faults omit Ordovician and upper Cambrian stratigraphy. The interactions of fault traces with topography, combined with multiple 3 point-problems calculated along their length (Long et al., 2014) demonstrate their steep eastward dip, which refutes the older thrust fault interpretation.

Another high-offset structure that has had varying interpretations is the Pinto Summit fault (Lisenbee, 2001), which strikes approximately along Highway 50, and places Permian rocks against Silurian rocks. This fault has been interpreted as a down-to-the-east normal fault (Nolan et al., 1974; Lisenbee, 2001) and a top-to-the-west reverse fault (Taylor et al., 1993). However, the configuration of fault traces with respect to topography on the north and south ends of the map area, combined with the results of 3 point-problems (Long et al., 2014), define a steep (65–75˚) westward dip, which refutes the thrust fault interpretation.

MINERAL DEPOSITS

The area around Eureka has been a center of mining and mineral exploration since the discovery of silver-gold-lead ore in 1864 at Ruby Hill, which is located north of the map area, southwest of the town of Eureka (Nolan, 1962, Nolan and Hunt, 1968). Most of the mineral deposits occur in Cambrian and Ordovician rocks near the central axis of the Eureka culmination described below. For over 100 years, most production in the Eureka district came from mainly oxidized, polymetallic carbonate replacement deposits, from which 1,266 tonnes (39 million ounces) of silver, 53.6 tonnes (1.65 million ounces) of gold, 285,000 tonnes (313,000 tons) of lead, 910 tonnes (1000 tons) of copper, and 6,360 tonnes (7,000 tons) of zinc were produced (Nolan, 1962, Nolan and Hunt, 1968). In the late 1970s and 1980s, disseminated, carbonate-hosted gold ores, similar to Carlin-type gold deposits on the Carlin Trend and elsewhere in northeastern Nevada (Hofstra and Cline, 2000; Cline et al., 2005), were discovered and mined in Windfall and Ratto canyons in the map area. In the 1990s, the much larger Archimedes Carlin-type gold deposit near the town of Eureka was discovered and put into production. From 1976–2012, production from these Carlin-type deposits in the Eureka district was approximately 44.9 tonnes (1.38 million ounces) of gold (NBMG, 2014).

Mineral deposits in the map area are summarized in table 4 (note: ***Table 4****. Summary of ore deposits in the map area, is included in a separate file*). Both polymetallic carbonate replacement deposits and Carlin-type gold deposits are present. In addition, numerous zones of hydrothermal alteration and mineral occurrences occur in the area, many of which have been explored and drilled. The polymetallic deposits occur as gossanous replacement bodies and fissure fillings in dolomite or limestone. Except for local jasperoid development, there is no macroscopically-recognizable alteration halo in the carbonate host rocks. Minor silver, gold, and lead were produced from these deposits, mainly in the late 1800s. They also contain zinc. The deposits that are hosted in Cambrian and Ordovician rocks near the central axis of the Eureka culmination include the Burning Moscow, Fourth of July, Geddes-Bertrand, Hoosac, and Page and Corwin mines. They resemble the polymetallic ores in the Ruby Hill and Mineral Point area in the northern part of the district. The ores in the north part of the district are spatially associated with, and interpreted to be the same age as, Late Cretaceous intrusions dated between 105–108 Ma (Nolan, 1962; Vikre, 1998; Mortensen et al., 2000). No Cretaceous intrusions were dated near the polymetallic deposits in the map area. Eocene dacite and rhyolite porphyry dikes of the Ratto Springs dacite and Pinto Peak Rhyolite are present but are not closely associated spatially with the polymetallic deposits.

Other polymetallic deposits occur along the western edge of the Eureka culmination and further west in the McCulloughs Butte area, the largest being the Reese and Berry and the Dugout Canyon mines. These contain less gold, copper, and lead and more zinc than the deposits further east. The mineralization at both mines occurs in quartz veins in silicified Pogonip Group limestones. The Reese and Berry and Dugout Canyon mines and numerous nearby mineral occurrences are likely distal deposits related to the emplacement of Late Cretaceous two-mica intrusions at McCulloughs Butte and Rocky Canyon.

At McCullough's Butte, Barton (1987) reported three muscovite and one biotite K-Ar dates that range from 83.8±1.9 to 47.5±1.0 Ma; the oldest age is probably the best estimate of the time of emplacement. A large fluorine resource of more than 109 million tonnes (120 million tons) grading 10% CaF_2 occurs at McCulloughs Butte (NBMG, 2014). The resource is mainly hosted by Ordovician Pogonip Group limestone and contains appreciable zinc and beryllium and minor amounts of molybdenum, tungsten, and tin in addition to fluorite (Barton, 1982). Barton (1982) documented a large, zoned hydrothermal system centered on the resource. The resource is zoned outward from proximal fluorite-bearing pegmatites, greisen, and skarn associated with granite porphyry dikes to veins with fluorite±sphalerite±molybdenite±beryl±pyrite to distal quartz-carbonate veins with barite and Sb-sulfosalts, such

as what is seen at the Reese and Berry Mine. Pogonip Group limestone is pervasively dolomitized within the zoned system for a distance of almost 3 km from the outcrops of Cretaceous dikes.

In Rocky Canyon, a core hole drilled in 1963 by Newmont Mining Corp., targeting a porphyry molybdenum system, intercepted multiple greisenized, two-mica granite dikes and skarn and hornfels in Secret Canyon shale. Molybdenite-bearing zones were encountered, but the target was not pursued. As part of this study, sample NMC-609C-939' was collected from the core hole. Abundant, large, euhedral zircons from the sample gave a TuffZirc $^{206}Pb/^{238}U$ age of 87.42+0.78/-0.82 Ma and concordia intercept age of 86.04±0.84 Ma (table 1).

Polymetallic ore was mined mainly for silver and lead from the Queen and Fairplay deposits at the southeastern end of the map area (Nolan et al, 1974). Several shafts and adits were developed in limestone and dolomite of the Devonian Devils Gate Limestone and the Bay State member of the Devonian Nevada formation. Ores in these host rock units were mainly replacement bodies and quartz veins.

As pointed out by Nolan (1962), carbonate-hosted disseminated gold ore mined underground from the Windfall Mine (in the map area) sporadically from 1908 until 1951 was quite different in that it contained realgar and low concentrations of silver and base metals. This led to exploration, starting in 1968, and discovery of additional gold ore. Approximately 90,000 ounces of gold were produced from three open pits (Windfall, Rustler, and Paroni) periodically from 1976 until 1989. The gold ore occurred mainly in sanded (partly de-dolomitized) Hamburg dolomite along its hanging wall contact with Dunderberg Shale and in jasperoid bodies in the Hamburg (Wilson and Wilson, 1986). Ore is mostly oxidized, but where not weathered is associated with fine-grained pyrite and local realgar (mainly in the Dunderberg Shale). It contained high concentrations of arsenic and mercury, typical of Carlin-type gold deposits in Nevada. The pits are aligned north-northwest along the Hamburg-Dunderberg contact, spaced over a distance of 2.3 km.

Another zone of Carlin-type gold deposits in the map area occurs south of Rocky Canyon, where large bodies of jasperoid are aligned north-northwest over a distance of more than 2 km on Ratto Ridge, west of Ratto Canyon. Systematic gold exploration of the area began in 1978, resulting in the partial development of several gold deposits, one of which, Lookout Mountain, was mined in 1987 and 1988, producing 17,700 ounces of gold. The area has experienced several exploration campaigns since. Most recently, Timberline Resources Corporation released a measured and indicated resource estimate of 28,949,000 tons grading 0.018 ounces per ton, and containing 508,000 ounces of gold. Most of the ore occurs in a large hydrothermal collapse breccia along and in the footwall of the Lookout Mountain normal fault that places Devonian rocks against Cambrian rocks. The breccia formed by dissolution of carbonate rocks in the Cambrian Hamburg dolomite, Dunderberg shale, and to a much lesser extent, in Devonian rocks. The breccia has been variably silicified, forming jasperoid. The gold-mineralized rock is mostly oxidized. Unweathered gold-mineralized Dunderberg Shale is characterized by arsenian pyrite, arsenopyrite, and realgar associated with quartz-kaolinite alteration.

Another Carlin-type occurrence is the Oswego mine, where disseminated gold ore was mined in the 1800s along a normal fault that placed Secret Canyon Shale over Eldorado dolomite (Nolan et al., 1974). Realgar and orpiment were locally present in the ore. Drilling by Amselco Minerals indicated gold grades did not persist at depth (Steininger et al., 1987).

AGE OF CARLIN-TYPE GOLD DEPOSITS

Where age control is available, Carlin-type gold deposits in Nevada are demonstrated to have formed between 42 and 34 Ma (Hofstra et al., 1999; Arehart et al., 2003; Cline et al., 2005; Ressel and Henry, 2006). Direct ages of the Carlin-type deposits in the Eureka district are not available, although determining their age was a goal of this project. Constraints on their age come mainly from their relationships with igneous rocks; the Carlin-type deposits are younger than Cretaceous intrusions, but their age relative to the Eocene rocks remains ambiguous.

At the east end of the Archimedes deposit, arsenian pyrite associated with quartz-kaolinite alteration with local orpiment and realgar clearly cross-cut and replace intrusions altered to quartz-sericite-pyrite, skarn, marble, and sphalerite-rich mineralization that occurs along the contact between Cambrian and Ordovician carbonates and the Late Cretaceous Graveyard Flats granitic porphyry stock (Dilles et al., 1996; Margolis, 1997; Hastings, 2008). The stock has a U-Pb zircon date of 106.2 ± 0.2 Ma (Mortensen et al., 2000).

Russell (2000) pointed out that north-south faults (e.g., Holly and Jackson fault systems) pre-date Carlin-type gold mineralization at Archimedes. The Holly and Jackson fault systems in the Archimedes area are analogous to the normal faults documented in the map area (e.g., Hoosac, Dugout Tunnel, Lookout Mountain, and Pinto Summit faults), which are bracketed between ~86 and ~37 Ma as reported below. The Lookout Mountain deposit clearly post-dates the major displacement on the Lookout Mountain fault.

None of the Cenozoic igneous rocks dated in this or previously published studies host ore or contain sulfide or other definite hydrothermal minerals in the Eureka district. The greatest alteration consists of plagioclase destruction and Na_2O loss in several Ratto Spring, Pinto Peak, and Target Hill rocks (e.g., fig. 3). The most altered rocks are represented by samples H10-62 (37.43±0.03 Ma), a plagioclase-hornblende-biotite dacite breccia block from

the Rustler pit; H11-135 (36.58±0.05 Ma), a coarsely porphyritic garnet-bearing rhyolite dike from near the Page-Corwin Mine; H11-137 (not dated but assigned to the Target Hill rhyolite), a coarsely porphyritic rhyolite dike ~1 km south of the Page-Corwin mine; H11-130 (35.86±0.05 Ma), a dike from the divide between the upper ends of New York and Windfall Canyons; and, based on Au, As, and Hg contents, H11-138 (37.28±0.21 Ma), a porphyritic dacite breccia at the Lookout Mountain pit. Plagioclase in the first four samples is altered, and the rocks have lost almost all their Na_2O; H11-135 and 137 have gained K_2O (fig. 3). Plagioclase and matrix are altered to montmorillonite in H11-138; the dacite in the Rustler pit and similar rock in the Windfall pit contain kaolinite as determined from SWIR spectral data. In two of the five samples that contained hornblende, it is altered to unidentified clay and calcite in H10-62 and unaltered in H11-138. Biotite, present in all samples, and sanidine in the rhyolites, are unaltered.

The porphyritic dacite at the south end of the Lookout Mountain pit, represented by H11-138, overlies what appears to be a regolith developed on weakly altered Cambrian Dunderberg Shale. The base of the dacite is marked by a 0.5 meter thick zone of white clay, determined from SWIR spectral data to be montmorillonite. The dacite assays as high as 16 ppb Au, 212 ppm As, and 4 ppm Hg. Dunderberg Shale directly underlying the dacite assays 6 ppb Au, 926 ppm As, and 4.2 ppm Hg. The previously described equivocal dike in the Lookout Mountain pit has not been assayed but contains fragments of jasperoid; thus it is either syn-ore or post-ore.

Wilson and Wilson (1986) reported that dacites in the Windfall and Rustler pits are altered. Alteration appears to decrease upward away from the underlying contact with mineralized Paleozoic rocks. This is especially apparent in transects on the west wall of the Rustler pit from mineralized Cambrian Hamburg dolomite upward to white-clay altered volcanic rocks with local opal to weakly altered volcanic rocks with fresh biotite. Drilling results of these dacite breccias from the 1970s indicated gold assays less than detection (<68 ppb); however, they were reported to contain elevated arsenic and mercury (Wilson and Wilson, 1986). Using a Niton portable XRF analyzer in this study, a transect showed the following upward attenuation of arsenic concentrations over a ~6 meters vertical extent: 1) 636 ppm As, Cambrian Hamburg jasperoid; 2) tan to white clay-altered dacite containing, going up the pit wall, 737 ppm As, 144 ppm As, 46 ppm As, 23 ppm As, and ending in; 3) a greenish, weakly altered dacite breccia with fresh biotite, 10 ppm As. Mercury concentrations using the portable XRF ranged up to 56 ppm.

The combined data are consistent with either hypogene or supergene alteration of the Eocene rocks. The clay alteration to montomorillonite and kaolinite and the strongly anomalous arsenic and mercury concentrations at Lookout Mountain and Rustler are consistent with hydrothermal alteration related to formation of the Carlin-type gold mineralization. If plagioclase destruction and Na_2O loss indicate hydrothermal alteration, then that alteration is younger than ~35.9 Ma, the age of several Target Hill rhyolites that have undergone such alteration. Further, if any of the Eocene rocks are pre-mineral, Carlin-type gold mineralization was likely at shallow depths, possibly only a few hundred meters based on estimates of the thickness of the Ratto Springs dacite. Lack of alteration in other Eocene rocks could indicate only that hydrothermal fluids did not reach them at their shallow depths, at most a few hundred meters below the paleosurface at ~37–36 Ma, as well as lesser reactivity of rocks composed mostly of quartz and feldspar.

Alternatively, supergene alteration from acidic fluids released by oxidation of pyrite and other sulfides in the mineralized Paleozoic rocks could account for the mineralogical and chemical characteristics. Such supergene acidic fluids would carry As, Hg, and Au, and their interaction with igneous rocks would be facilitated by location of dikes surrounded by Paleozoic rocks and of the volcanic rocks in deep paleocanyons eroded into and topographically below adjacent Paleozoic rocks. For example, sample H10-62 is from the wall of the Rustler pit at an elevation of 2353 m, far below adjacent Paleozoic rock in Hamburg Ridge (2593 m) and Hoosac Mountain (2597 m). Acidic fluids formed by oxidation of the adjacent rocks would have drained into the topographically low areas where the volcanic rocks had been deposited, although the fluids would have been variably neutralized before reaching the igneous rocks. If alteration is supergene, neither the age nor the depth of Carlin-type mineralization is as tightly constrained.

GEOLOGIC HISTORY

The map area is situated in a region of Nevada that has occupied a diverse range of tectonic settings that have evolved through the Phanerozoic (e.g., Dickinson, 2006). This tectonic development is preserved in a rock record that spans the Paleozoic, Mesozoic, and Cenozoic.

From the late Neoproterozoic to the Devonian, the Cordilleran passive margin sequence, a westward-thickening section of clastic and carbonate rocks, was deposited on the rifted North American continental shelf in what is now eastern Nevada and western Utah (e.g., Stewart and Poole, 1974), and Eureka was situated near the distal, western margin of the shelf (Cook and Corboy, 2004). In the map area, the exposed part of the passive margin sequence is 4.7 km thick, and consists of lower Cambrian clastic rocks, including the Prospect Mountain Quartzite, and a middle Cambrian to Devonian carbonate platform section dominated by limestone and dolomite, with lesser quartzite and shale.

During the Mississippian, the Roberts Mountains allochthon, composed of distal slope and rise sediments,

was thrust to the east over the western edge of the continental shelf during the Antler orogeny (e.g., Burchfiel and Davis, 1975; Dickinson, 1977; Speed and Sleep, 1982). The map area lies in the footwall of the Roberts Mountains thrust, the basal structure of the Antler event, which is exposed ca. 10 km north of the map area in the Mountain Boy Range (Bentz, 1983; Drake, 1978). During the Antler orogeny, the map area was the site of synorogenic deposition of Mississippian clastic sediments that were sourced from the Roberts Mountains allochthon, in the flexural foreland basin that subsided in front of the growing orogenic belt (e.g., Poole, 1974; Smith and Ketner, 1977; Poole and Sandberg, 1977). Rock units of the Antler foreland basin include the Dale Canyon Formation and Chainman Shale (note: rocks mapped as Chainman Shale in this study are likely equivalent to the Gap Wash Formation of Trexler et al. [2003], and may pre-date rocks mapped as Chainman Shale further east and south in Nevada). The overlying Diamond Peak Formation is interpreted to represent deposition in the Antler successor basin, either representing late-stage deformation associated with the Antler orogeny, or a distinctly younger deformation event (Trexler et al., 2003).

During the Pennsylvanian and early Permian, eastern Nevada experienced a protracted series of deformation, erosion, and deposition events that record contractional deformation of the western Laurentian margin outboard of the time-equivalent Ancestral Rockies orogenic event recorded in Utah (Trexler et al., 2004). These deformation events are recorded by unconformity-bound packages of carbonate and clastic rocks, which in the map area consist of the Pennsylvanian Ely Limestone and Permian Carbon Ridge Formation. Notably, the Ely Limestone, which is up to ~1 km thick in areas of eastern Nevada (e.g., Rich, 1977), is only a few hundred meters thick in the southern Diamond Mountains, and pinches out in the central part of the map area.

During the Jurassic and Cretaceous, contractional deformation, plutonism, and metamorphism associated with Cordilleran orogenesis took place across Nevada and western Utah, and are attributed to deformation of the North American plate above an eastward-directed, Andean-style subduction zone (e.g., Burchfiel and Davis, 1975; Allmendinger, 1992; DeCelles, 2004). The map area lies within a large hinterland region situated between the Jurassic Luning-Fencemaker thrust belt in western Nevada (e.g., Oldow, 1984; Wyld, 2002) and the latest Jurassic–Cretaceous Sevier fold-thrust belt in western Utah (e.g., Armstrong, 1968; DeCelles, 2004). Much of this hinterland region lacks surface-breaching thrust faults (Armstrong, 1972; Gans and Miller, 1983; Long, 2012); however, the map area lies within the central Nevada thrust belt (CNTB), a NNW-trending zone of contractional structures that branch off of the type-Sevier thrust belt in southern Nevada (Taylor et al., 2000; Long, 2012). In the map area, CNTB structures include the blind Ratto Canyon thrust, which is defined by a Cambrian over Silurian relationship observed in drill holes, the east-vergent Prospect Mountain/Moritz-Nager thrust, and several N-striking, map-scale folds (Long et al., 2014). In addition, retro-deformation of overprinting extensional faulting reveals the existence of the Eureka culmination, a regional-scale anticline that trends through the map area (Long et al., 2014). The culmination is interpreted as a fold that grew contemporaneous with slip on the Ratto Canyon thrust at depth. The type-section of the Early Cretaceous Newark Canyon Formation was deposited in a piggyback basin on the eastern limb of the culmination as it grew (Long et al., 2014), and therefore defines the probable Aptian age of CNTB deformation in the Eureka region.

During the Cretaceous, granitic rocks of two known ages intruded Paleozoic rocks in the Eureka area (Mortensen et al., 2000; Vikre, 1998; Nolan et al., 1971). The only outcrops in our map area are dikes of two-mica granite that intrude Antelope Valley formation at McCullough's Butte and are associated with fluorite-rich skarn (Barton, 1987). Barton (1987) reported three muscovite and one biotite K-Ar dates that range from 83.8±1.9 to 47.5±1.0 Ma; the oldest date is probably the best estimate of the time of emplacement. Multiple two-mica granite dikes were encountered in a drill hole in Rocky Canyon. Sample NMC-609C-939' yielded abundant, large, euhedral zircons that give a TuffZirc $^{206}Pb/^{238}U$ date of 87.42+0.78/-0.82 Ma and concordia intercept date of 86.04±0.84 Ma (table 1).

Numerous granitic stocks and sills crop out or have been encountered by drilling in the northwestern part of the Eureka district (fig. 1). These rocks are metaluminous, biotite-hornblende-bearing granodiorites typical of Cretaceous plutons throughout northern Nevada. In the Eureka district, U-Pb zircon and $^{40}Ar/^{39}Ar$ dates of granitic rocks cluster around 106 Ma (Mortensen et al., 2000; Vikre, 1998). The granodiorites were the heat source for the Ag-Pb-Zn-Au replacement and vein deposits that were episodically mined from 1866 to the 1960s (Nolan, 1962; Vikre, 1998).

After construction of the Eureka culmination, the map area underwent ca. 7–8 km (45–50%) of extension, accommodated by two distinct sets of normal faults, which both pre-date Late Eocene (ca. 37 Ma) volcanism (Long et al., 2014): 1) an older set consisting of the down-to-the-east Hoosac fault system and down-to-the-west Reese and Berry detachment system, which have offset magnitudes between 2–5 km; and 2) a younger set consisting of high-angle, down-to-the-west normal faults with offset magnitudes between 2–4.5 km, including the Dugout Tunnel, Lookout Mountain, and Pinto Summit faults. Motion on faults of set 2 was accompanied by up to 20–30° of eastward tilting, as estimated by the dip of the Late Cretaceous to late Eocene conglomerate on Hoosac Mountain. Faults of set 1 are cut and tilted by faults of set 2, and faults of set 2 cut a Late Cretaceous (ca. 86 Ma) contact aureole and tilt the conglomerate on Hoosac Mountain that has a Late Cretaceous (ca. 72 Ma) maximum deposition age (Long et al., 2014).

During the late Eocene and Oligocene, the Great Basin ignimbrite flareup, an episode of silicic volcanism, swept from northeast to southwest across Nevada (e.g., Armstrong and Ward, 1991; Best and Christiansen, 1991; Henry, 2008; Best et al., 2009). In the map area, rocks of this episode include late Eocene (ca. 37–35 Ma) silicic lavas, tuffs, shallow intrusive rocks, and associated volcaniclastic and sedimentary rocks, including the Ratto Spring dacite, Pinto Peak Rhyolite, Richmond Mountain dacite, Target Hill rhyolite, and Basalt Peak andesite (see discussion of Eureka volcanic center above). Notably, the modern topographic lows of several prominent canyons incised into Paleozoic bedrock, including Oxyoke, Rescue, and Ratto canyons, contain exposures of late Eocene volcanic rocks and air-fall tuffs, indicating that they must have been incised by the late Eocene.

From the Neogene to the present, Nevada and Utah have been the site of regional extensional tectonism that formed the Basin and Range Province. Widespread, large-magnitude, upper-crustal extension began in the early Miocene (~17.5 Ma) (e.g., Dickinson, 2006), and by ~10 Ma either transitioned into, or was followed by a separate episode of, lower magnitude extension that formed the modern Basin-and-Range topography (e.g., Dickinson, 2002; Colgan and Henry, 2009). In the map area, the majority of high-throw normal faults pre-date late Eocene volcanism (Long et al., 2014). However, normal faults that bound modern topographic basins, including the Spring Valley fault, and the fault bounding the eastern end of the Diamond Mountains, are likely Neogene in age, although no precise timing constraints can be placed on their motion age. Notably, the map patterns of late Eocene rocks, including km-scale lava flows and dome systems, widely-distributed air-fall tuffs, and associated sedimentary deposits, as well as the map-scale geometry of the basal late Eocene unconformity in cross section, indicate that only minor (≤10°) tilting or vertical throw on normal faults has taken place in most of the map area since the Late Eocene (Long et al., 2014).

DESCRIPTION OF MAP UNITS

Quaternary Deposits

Qm Artificial fill, including mine dumps Piles of discarded, broken rock from mining; from recent open-pit mining at Lookout Mountain and Windfall Canyon.

Qa Alluvium Unconsolidated, poorly-sorted silt, sand, and gravel deposited in gently-sloping modern drainages.

Qt Terrace deposits Unconsolidated silt, sand, and gravel deposited that have been incised by the modern stream in Windfall Canyon, and are overlapped by modern alluvium.

Qf Alluvial fan deposits Unconsolidated to poorly-consolidated silt, sand, and gravel deposited by debris-flow processes at the mouths of modern drainages; forms broad, gently-sloping alluvial aprons in Spring Valley and the eastern flank of the Diamond Mountains.

Qc Colluvium Unconsolidated, locally-derived, slope-mantling deposits of angular pebble- to boulder-size clasts. Colluvium is particularly common in areas downslope from competent Paleozoic units such as Eureka Quartzite (Oe), and in the vicinity of poorly-consolidated Tertiary volcanic units.

Qls Landslide deposits Two landslide deposits are mapped, one the east flank of south Lookout Mountain, which is composed of map units Cd and Cwb, which have been transported a short distance downhill toward the east, and the other on the eastern flank of Hoosac Mountain, where a concentration of boulders comprised of map unit Oe has slumped down toward the east.

Quaternary–Tertiary Deposits

QTg Capping gravel Gravel mostly composed of Paleozoic rocks, especially quartzite, with lesser limestone and dolomite, and sparse rhyolite and andesite. Mostly exposed as a lag of rounded boulders and less commonly as calcite-cemented gravel that caps ridges in the western inset map area. Similar in rock type and geomorphic expression to, and possibly equivalent to, gravel mostly composed of mixed Paleozoic rocks (Tgm) in the northern part of the map area. Deeply dissected and perched above modern alluvium, but age is otherwise uncertain.

Tertiary Rocks

Tmh Magpie Hill Basalt Dark gray, massive to vesicular, alkali-olivine basalt lava flow. Mostly aphyric with sparse plagioclase megacrysts to 2.5 cm long. Crops out only in inset area in southern part of Rescue Canyon, where it is a single lava flow about 30 m thick. Age: 20.1±0.6 (K-Ar whole rock) on a sample from ~2 km southeast of Magpie Hill (fig. 2) and 20.7±0.8 Ma (K-Ar plagioclase) on a sample from an unknown location (Nolan et al., 1974).

Tmc Conglomerate below Magpie Hill Basalt Poorly cemented and very poorly exposed gravel containing rounded clasts of Pancake Summit Tuff and other porphyritic volcanic rocks up to about 20 cm in diameter. Crops out only in inset map area in southern part of Rescue Canyon, where it underlies Magpie Hill Basalt.

Tnh Nine Hill Tuff Red-brown, sparsely porphyritic, devitrified, rhyolitic ash-flow tuff that grades upward from poorly- to moderately-welded. Contains 2 to 5% phenocrysts consisting mostly of sanidine to 1.5 mm,

sparse quartz to 1 mm, and probable altered plagioclase to 1 mm. Common moderately-flattened pumice to 5 cm long. Crops out only in eastern inset area, in southern part of Rescue Canyon, where it is about 5 to 20 m thick and filled in against eroded Pancake Summit Tuff in the canyon cut into Paleozoic rocks. Age: 25.38±0.08 Ma, which is an average of 12 $^{40}Ar/^{39}Ar$ sanidine analyses in central and western Nevada and eastern California (Henry and John, 2013).

Tps Pancake Summit Tuff Abundantly porphyritic, rhyolitic ash-flow tuff that grades upward from a light-gray, poorly welded, locally vitrophyric base to dark red-brown, densely welded, devitrified top. Crops out only in Rescue Canyon, where it is as much as 85 m thick and filled a steep canyon cut into deeply eroded Paleozoic rocks and undivided pyroclastic deposits (Trt). Phenocrysts are subequal amounts of smoky quartz to 3 mm, variably adularescent sanidine to 4 mm, lesser plagioclase to 2 mm, and minor biotite and hornblende. Sparse, faint pumice to 3 cm long. Named tuff of Pancake Summit by Gromme et al. (1972) and formalized to Pancake Summit Tuff (Nolan et al., 1974), it erupted from the Allison Creek caldera in the northern Monitor Range ~40 km west of the map area (Best et al., 2013). Age: 35.36±0.07 and 35.40±0.06 Ma; $^{40}Ar/^{39}Ar$, sanidine, based on two samples from Pancake Summit (fig. 1; Henry and John, 2013).

Tpc Conglomerate below Pancake Summit Tuff Very poorly exposed conglomerate consisting of subrounded boulders of mixed volcanic rocks up to 40 cm in diameter. Exposures consist of boulder lag with no matrix.

Late volcaniclastic and sedimentary deposits A sequence of mostly coarse to locally fine clastic sedimentary rocks that accumulated in the valley between Hoosac Mountain and Woodpeckers Peak. Emplacement of the Pinto Peak dome complex created a possibly closed basin north of the complex. The deposits record continued erosion of surrounding Paleozoic rocks and of the volcanic and intrusive rocks, probably partly during the waning stages of local igneous activity but mostly after local magmatism ceased. The different map units are distinguished on the basis of stratigraphy and clast type, with the proportion of igneous clasts generally decreasing and of Paleozoic sedimentary clasts increasing upwards. Distinct differences in clast type and abundance between the different units suggest that different surrounding high areas fed alternately into the basin through time. Contacts are poorly exposed.

Tgm Gravel mostly composed of mixed Paleozoic rocks The stratigraphically highest unit caps the highest ridges north of Pinto Peak and is dominated by rounded clasts of quartzite and limestone, both to 1.2 m, with less than 10% mixed volcanic rocks. At most about 15 m thick. Similar to and possibly equivalent to capping gravel (QTg), and age is similarly uncertain.

Tgv Gravel mostly composed of mixed volcanic rocks Coarse, poorly cemented gravel consisting of a lag of igneous rocks representing all the major rock types of the area that are up to 2 m in diameter. Up to about 40 m thick. Distinguished from the upper part of the Ratto Spring coarse volcaniclastic deposits (Trsv), which it commonly rests on, by the presence of Paleozoic clasts and post-Ratto Spring volcanic clasts.

Tcrm Gravel mostly composed of Basalt Peak andesite Coarse, poorly cemented gravel dominated by a lag of aphyric Basalt Peak andesite to 1.2 m. Other clasts include Paleozoic quartzite to 1 m and limestone to 70 cm, porphyritic dacite to 15 cm, and porphyritic rhyolite to 12 cm. Sparse outcrops indicate some tuffaceous matrix and lenses. Up to about 50 m thick. Dominance of aphyric andesite clasts indicates source to north for deposits north of Pinto Peak. Also forms east-dipping ridge caps in the northeastern part of the map area, where it is derived from the large area of Basalt Peak andesite outcrop at and north of Basalt Peak. Previously mapped as in situ Basalt Peak andesite but definitely reworked.

Tcl conglomerate composed of Paleozoic limestone clasts Several discontinuous lenses of conglomerate about 5 to 20 m thick, predominantly composed of well-rounded Paleozoic limestone clasts up to 50 cm in diameter, locally with lesser amounts of quartzite and various volcanic rocks. Calcite-cemented where matrix is exposed. Lenses occur mostly in lower parts of the sequence, but one overlies gravel mostly composed of Basalt Peak andesite (Tcrm).

Tsc Sandstone Massive to thick-bedded, calcite-cemented, coarse sandstone and minor pebble-cobble conglomerate, probably at most about 10 m thick. Lowermost sandstone has abundant pumice, which disappears upwards. Conglomerate makes channel lenses with clasts of volcanic rocks and Paleozoic sedimentary rocks to 10 cm in diameter.

Eureka Volcanic Center

Tba Basalt Peak andesite Thick sequence of dark, generally black, massive to highly vesicular, aphyric to very sparsely porphyritic andesite lavas. Sparse

phenocrysts consist of plagioclase and lesser ortho- and clinopyroxene less than 1 mm in diameter. Crops out along northeast edge of map area and extensively to north and northwest toward Richmond Mountain (Nolan et al., 1974), where shallow intrusions are also present. Aligned vesicles generally point towards Basalt Peak, which may have been a source for some flows. Age: 35.58±0.18 and 35.67±0.16 Ma; $^{40}Ar/^{39}Ar$, two matrix splits of H11-77 in northeast part of map. Also 35.36±0.24 Ma, $^{40}Ar/^{39}Ar$ isochron date of matrix from H11-107 from the near the top of Richmond Mountain.

Target Hill rhyolite The younger of two similar rhyolite suites that consist of lava domes, coarse marginal breccias around domes, pyroclastic-flow, -fall, and -surge deposits, and dikes. Named rhyolite of Target Hill by Nolan et al. (1971) for Target Hill next to Eureka ~4 km north of the north edge of the map area, then assigned to the formal Pinto Peak Rhyolite by Nolan et al. (1974) and Blake et al. (1975). Precise $^{40}Ar/^{39}Ar$ dating shows that Target Hill rhyolites intruded at ~35.9 Ma and are distinctly younger than Pinto Peak Rhyolites, which are ~36.6 Ma. Target Hill rhyolites contain 15 to 20% phenocrysts of quartz and sanidine, lesser plagioclase, minor biotite, and in a few less silicic samples, traces of hornblende and/or orthopyroxene (table 2). This assemblage is similar to that of Pinto Peak Rhyolites but is mostly more finely porphyritic, with phenocrysts all ≤2.5 mm. Also, garnet has not been found in any Target Hill rocks in the map area or near Target Hill at Eureka. However, rhyolite intrusions at Mount Hope and Garden Hill, ~40 km northwest of Eureka, have ages indistinguishable from Target Hill rocks and do contain garnet. Chemical analyses show that Target Hill rhyolites range to lower SiO_2 and even the highest SiO_2 rocks are slightly less evolved than Pinto Peak Rhyolites, with higher TiO_2, FeO, Sr, Zr, Hf, and LREE and lower Rb, Y, Nb, Ta, HREE, and aluminum saturation indices; the lower saturation index is consistent with the absence of garnet.

Ttr Lava domes Lava domes are interpreted to be extruded almost directly below their outcrop on the basis of steep contacts with adjoining coarse breccia, steep commonly concentric flow bands, and elevation above surrounding rocks that indicate they extruded well above any country rock. Target Hill north of the map area is the best example. Marginal vitrophyre is developed in the Target Hill and Grey Fox Peak domes. Age: 35.97±0.03 Ma, $^{40}Ar/^{39}Ar$, sanidine, H11-99, Target Hill; 35.4±0.2, U-Pb, zircon, 96-M-205, Purple Mountain, a part of Target Hill (Mortensen et al., 2000); 35.98±0.04 Ma, $^{40}Ar/^{39}Ar$, sanidine, H11-136, south edge of map area; 35.78±0.07 Ma, $^{40}Ar/^{39}Ar$, sanidine, H11-143, Grey Fox Peak south of map area.

Ttrx Coarse breccia Breccia consisting of coarse, commonly vitrophyric clasts of porphyritic rhyolite of the adjoining lava dome in a poorly to locally well-exposed matrix of finer clasts. Clasts range up to at least 5 m in diameter. Breccia capping hill 7142 south of Pinto Basin has a well-exposed feeder dike but no adjoining lava dome, which suggests extrusion stopped before sufficient magma erupted to develop a dome.

Ttt Pyroclastic-flow, fall, and surge deposits Heterogeneous mix of massive to bedded tuffs that are mostly nonresistant, and make numerous small and a few larger outcrops, especially in the western inset map area in lower Ratto Canyon. Massive, unsorted units are white (rhyolitic) to light brown (dacitic) pyroclastic-flow deposits (ash-flow tuffs) up to about 15 m thick. Most tuffs are poorly to moderately to rarely densely welded and show little welding zonation. Pumice up to 8 cm long is abundant; rhyolitic to dacitic lithic fragments up to 4 cm in diameter are sparse to as much as 15% by volume. Pyroclastic-fall and surge deposits mostly make 0.2 to 2 m thick layers separating flow deposits. Fall deposits are planar bedded, moderately well sorted, and contain abundant pumice and lithic fragments. Surge deposits are planar to cross bedded, poorly sorted, and locally contain abundant, commonly imbricated lithic fragments. All tuffs contain 25 to 40% phenocrysts of plagioclase, quartz, and biotite, with the addition of sanidine in rhyolites and hornblende, and clino- and orthopyroxene in dacites. Age, all on dacite tuffs in ascending stratigraphic order in section in lower Ratto Canyon inset map area: 35.77±0.14 Ma, $^{40}Ar/^{39}Ar$, plagioclase, H11-64; 35.83±0.04 Ma, $^{40}Ar/^{39}Ar$, sanidine, H11-59; 35.91±0.16 Ma, $^{40}Ar/^{39}Ar$, biotite.

Ttrd Dikes Dikes of rhyolite to high-SiO_2 dacite are mostly 2 to 8 m wide and up to 500 m long, although most are too discontinuously exposed to determine length. Many dikes strike east and appear to have filled existing fractures in Paleozoic rocks. A well-exposed dike that fed the small area of breccia (Ttrx) at hill 7142 south of Pinto Basin widens upward from 2 to 6 m, has a sharp to irregular contact with surrounding tuff and breccia (Ttt, Ttrx), and partly domed intruded rock. Age: 35.96±0.05 Ma, $^{40}Ar/^{39}Ar$, sanidine, H11-140, Dunderberg Mine; 35.86±0.05 Ma, $^{40}Ar/^{39}Ar$, sanidine, H11-130, north of upper Windfall Canyon; 35.69±0.07 Ma, $^{40}Ar/^{39}Ar$, sanidine, BHSE-119-148, dike from drillhole south of Lookout Mountain.

Tirx Intrusive breccia Breccia consisting mostly of rhyolite and lesser dacite clasts in a

rhyolitic matrix makes several small spires in Hamburg Ridge west of Pinto Peak. Clasts of Paleozoic rocks range from absent to locally common. The breccia may be the fragmented upper part of a dike.

Trmv Richmond Mountain dacite Coarse volcaniclastic deposits consisting of blocks of abundantly porphyritic dacite up to 1 m in diameter in a matrix of finer dacite. Blocks are massive to vesicular and glassy to crystalline or devitrified; some are flow-banded. Most deposits are monolithic and contain some clasts with radial cooling joints, which shows that they are primary volcanic deposits. Rocks vary from finely to coarsely porphyritic, with phenocrysts mostly of plagioclase with biotite, hornblende, and sparse ortho- and clinopyroxene; sparse quartz is present in a few samples. Deposits in Ratto Canyon crop out in the bottom of the canyon, commonly at the same or lower elevation than some deposits of Ratto Spring dacites, which shows that the Ratto Spring dacite was deeply eroded before deposition of the Richmond Mountain dacite. The coarseness of deposits in Ratto Canyon indicates a probable nearby but unidentified source. The Richmond Mountain dacite on and around Richmond Mountain ~4 km north of the map area includes massive lavas, and the mountain itself is a hornblende dacite lava dome, which indicates the area was the source of much of the unit. Age: 36.16±0.07 Ma, $^{40}Ar/^{39}Ar$, plagioclase, H11-90, Ratto Canyon; 36.5±1.3 Ma, K-Ar, hornblende, PS88-6 (Blake et al., 1975).

Pinto Peak Rhyolite The older of two similar rhyolite suites that consist of lava domes, coarse marginal breccias around domes, lava flows, pyroclastic-flow, fall, and surge deposits, and dikes. Named for Pinto Peak in east-central part of map area. Pinto Peak rhyolites contain 15 to 25% phenocrysts of quartz and sanidine, generally lesser plagioclase, minor biotite, and commonly garnet. Distinguished from Target Hill rhyolite primarily by older age (36.6 Ma) and generally being more coarsely porphyritic, with sanidine and quartz phenocrysts up to 10 mm in diameter, presence of garnet phenocrysts, and more evolved composition, with higher Rb, Y, Nb, Ta, HREE, and aluminum saturation indices (consistent with the common presence of garnet) and lower TiO_2, FeO, Sr, Zr, Hf, and LREE. However, none of these characteristics may be diagnostic, because several dikes interpreted as part of the Target Hill rhyolite on the basis of compositional similarity to dated BHSE-119-148 (cuttings only so phenocryst size unknown) are coarsely porphyritic, and rhyolites that are of Target Hill age at Mount Hope and Garden Pass 40 km northwest of Eureka also contain garnet.

Tpr Lava domes Lava domes are interpreted to be extruded almost directly below their outcrop on the basis of steep contacts with adjoining coarse breccia, steep commonly concentric flow bands, and elevation above surrounding rocks that indicate they extruded well above any country rock. Pinto Peak is a complex of semi-coalesced lava lobes that probably intruded in a cone shape through surrounding breccia and tuff (Tprx, Tprt). None of the lava dome probably flowed significant lateral distances. Flow bands are roughly concentric and mostly steeply inward-dipping. Vitrophyre locally developed at contacts with intruded rocks. Generally more resistant and more continuous outcrop than coarse breccia (Tprx). Age: 36.69±0.04 Ma, $^{40}Ar/^{39}Ar$, sanidine, H11-86, top of Pinto Peak.

Tprx Coarse breccia Breccia consisting of coarse clasts of porphyritic rhyolite of the adjoining lava dome in a poorly to locally well-exposed matrix of finer clasts. Clasts range up to at least 5 m in diameter; vitrophyre is common. Forms steep, poorly to moderately well-exposed slopes adjacent to lava dome (Tpr). Where poorly exposed, random orientation of flow bands distinguishes from lava dome. Breccia probably formed by collapse off the lava dome surface as it extruded. Age: 36.63±0.05 Ma, $^{40}Ar/^{39}Ar$, sanidine, H11-80, flank of Pinto Peak.

Tprf Lava flow A small hill just north of the north flank of the Pinto Peak dome complex is interpreted to be a lava flow because it makes a flat, thin layer overlying siltstone and sandstone (Ts) and a feeder dike is nowhere exposed around the flow. Otherwise, similar to lava dome of Pinto Peak.

Tprt Pyroclastic-surge, fall, and flow deposits Heterogeneous mix of coarse to fine, generally layered to lesser massive pyroclastic deposits. Mapped only around the Pinto Peak lava dome where stratigraphic position below the lava dome is certain and only well exposed in lower Hoosac Canyon along the northeast flank. Mostly planar to irregularly bedded and containing abundant pumice to 5 cm and fragments of rhyolite to 10 cm. Locally much coarser with rhyolite fragments to 40 cm. Massive, probably ash-flow tuffs and fine, platy tuff, mostly as lag, are poorly exposed around Dale Canyon southwest of Pinto Peak.

Tprd Dikes Numerous dikes of mostly coarsely porphyritic rhyolite 3 to 25 m wide and up to 500 m long. Commonly flow-banded parallel to dike. Dikes cutting pyroclastic deposits (Tprt) bifurcate irregularly. Breccia of mixed rhyolite and country rock is developed at margin of dike near the Page-Corwin Mine. Age:

36.58±0.05 Ma, $^{40}Ar/^{39}Ar$, sanidine, H11-135, Page-Corwin area.

Tlc Older conglomerate of Paleozoic limestone Conglomerate consisting entirely of lag of well-rounded limestone clasts up to 90 cm in diameter. Exposed only along the northwest flank of Pinto Peak dome complex, where it underlies Pinto Peak Rhyolite lava dome, breccia, and pyroclastic deposits (Tpr, Tprx, Tprt) and overlies siltstone and sandstone (Ts). Probably about 30 to 40 m thick if flat-lying. Similar to but probably younger than breccia and conglomerate of Paleozoic rocks (Trsp), which is interlayered with Ratto Spring volcanic rocks and also contains some non-limestone Paleozoic clasts. Definitely older than "younger conglomerate of Paleozoic limestone" (Tcl), which overlies conglomerate mostly composed of Richmond Mountain Andesite (Tcrm).

Ts Siltstone and sandstone Very poorly exposed, white to very light gray, platy, tuffaceous fine sandstone and siltstone. Consists entirely of float of small chips up to about 5 cm long in light-colored soil. Found only in a band overlying lavas and volcaniclastic deposits of Ratto Spring rocks (Trs, Trsv) and underlying coarse breccia of Pinto Peak Rhyolite (Tprx) along the northwest flank of Pinto Peak dome complex, where it is probably as much as 40 m thick if flat-lying. Platy tuffaceous siltstone chips appear intermixed with uppermost Ratto Spring volcaniclastic rocks at 10° southwest dip, which suggests lower contact is gradational.

Undivided rhyolite Dikes and pyroclastic deposits whose age and affinity with either the Target Hill or Pinto Peak rhyolites cannot be determined. Their outcrop characteristics are similar to the deposits in the two rhyolite units.

Trd Dikes

Trt Pyroclastic-flow, fall, and surge deposits

Ratto Spring dacite A group of moderately to abundantly, and generally coarsely porphyritic, dacites that make coarse to fine volcaniclastic deposits and minor lavas; five $^{40}Ar/^{39}Ar$ dates average 37.3 Ma (table 1). Ratto Spring rocks contain 25 to 35% phenocrysts, mostly of plagioclase, that can be up to 8 mm in diameter, with significant biotite and hornblende (up to 1 cm long), minor orthopyroxene, and locally quartz.

Trs Lava flows Biotite-hornblende±quartz dacite lavas crop out in three small areas in the bottom of Ratto Canyon at the south edge of the map area, and on the northwest and northeast lowest flanks of Pinto Peak. Continuity of the massive lavas distinguishes them from volcaniclastic deposits. Age: 37.34±0.26 Ma, $^{40}Ar/^{39}Ar$, hornblende, H11-92, Ratto Canyon.

Trsv Coarse volcaniclastic deposits Coarse to some finer volcaniclastic deposits composed of dacite clasts commonly to 1 m in diameter and rarely to 5 m long in a matrix of finer volcanic material. Mix of primary, probably block-and-ash-flow and probable pyroclastic-surge and -fall deposits and reworked debris-flow deposits. Block-and-ash-flow deposits are very thick-bedded, massive, unsorted, matrix-supported, monolithologic, and commonly partly to entirely vitrophyric, and have blocks with radial cooling joints, which shows they cooled partly *in situ*. Deposits that have been definitely reworked are heterolithic, commonly entirely crystalline, and lack blocks with radial cooling joints. Faintly to well-bedded, thinly bedded, and coarse to relatively fine deposits are probably surge and fall deposits. Age: 37.14±0.12 Ma, $^{40}Ar/^{39}Ar$, plagioclase, H12-78, Windfall Canyon; 37.40±0.07 Ma, $^{40}Ar/^{39}Ar$, biotite, H11-88, upper Hoosac Canyon; 37.43±0.03 Ma, $^{40}Ar/^{39}Ar$, biotite, H10-62, Rustler pit; 37.28±0.21 Ma, $^{40}Ar/^{39}Ar$, hornblende, H11-138, Lookout pit.

Trsd Dikes dikes of probable Ratto Spring dacite age crop out in the Rustler and possibly Windfall pits and in Hoosac Canyon ~1.4 km northeast of Pinto Peak. In the Rustler pit, a north-striking, steeply west-dipping biotite-dacite dike intruded along the contact between Hamburg dolomite (Ch) and Dunderberg Shale (Cd), is ~10 m wide and at least 200 m long. A similar dike may be present about 800 m along-strike to the north in the south end of the Windfall pit. In Hoosac Canyon, an east-striking, approximately vertical, mostly glassy biotite-dacite dike intrudes coarse, moderately bedded volcaniclastic deposits (Trsv) and is up to 20 m wide and ~300 m long.

Trsp Breccia and conglomerate of Paleozoic rocks Angular to rounded clasts of commonly crinoid-bearing limestone and lesser chert-clast pebble conglomerate (probably Diamond Peak Formation; Mdp) form a lag in several areas south of Pinto Peak. Clasts are mostly 10 to 100 cm in diameter but one clast is 5 m in diameter. Although no matrix or bedding is exposed, the trace of lag boulders shows that these deposits are interbedded with coarse to fine Ratto Spring dacite volcaniclastic rocks (Trsv, Trst). The Paleozoic clasts may have been shed off an early dome in the Pinto Peak area. The outcrop of

Carbon Ridge Formation (Pcr) surrounded by Pinto Peak Rhyolite breccia deposits (Tprx) just west of the breccia-conglomerate lag is structurally out of place relative to nearby *in-situ* Paleozoic rocks to the south and is at least partly breccia also. Limestone in this outcrop shows relatively coherent north strike and steep east dip, which suggests it is a very large slump block.

Tj Jasperoid of unidentified protolith (alteration likely Cenozoic) Ridge- and cliff-forming, fine-crystalline jasperoid formed by silica replacement of Cambrian and Devonian carbonate protoliths. Localized along the Lookout Mountain fault at the top of Lookout Mountain. This alteration is likely syn-volcanic (late Eocene).

Ti Cenozoic(?) intrusions An irregular, dike- or sill-shaped body that cuts Hamburg dolomite in the Lookout Mountain pit and Lone Mountain Dolomite to the north. The rock is strongly bleached white in the pit and tan or light brown to the north, where it is as much as 10 m thick. Rock in the pit consists of very fine-grained quartz, clay, and opaque minerals. Petrography, chemical analysis, and zircon U-Pb dates suggest the rock in the pit is not igneous and possibly highly-altered fault gouge or breccia pipe. The origin of mapped Ti north of the pit is unknown.

KTc Latest Cretaceous to late Eocene conglomerate Thin- to medium-bedded, pebble to cobble conglomerate with brick-red matrix, rich in Paleozoic limestone clasts, with rare Oe clasts. Observed on Hoosac Mountain and in Windfall Canyon. Originally mapped as Early Cretaceous Newark Canyon Formation by Nolan et al. (1974); however, U-Pb detrital zircon geochronology (sample NV11DZ-017EU) reveals a ~72 Ma youngest population, defining a Late Cretaceous (Campanian) maximum depositional age (Long et al., 2014). The conglomerate is overlain by Ratto Spring dacite (Trsv; 37.14±0.12 Ma; sample H12-78) on the east flank of Hoosac Mountain, defining a late Eocene minimum depositional age. At least 30 m thick.

Mesozoic Rocks

Ki Late Cretaceous granite Two-mica granite dikes are exposed at McCullough's Butte, and are dated at 84±2 Ma (Barton, 1987). In addition, multiple two-mica granite dikes are intercepted in a drill hole (hole NMC609C on map) in northern Rocky Canyon, where they are associated with contact metamorphism of unit Cs to hornfels and skarn. A dike sampled from this hole (sample NMC609) yielded abundant, large, euhedral zircons that yield a TuffZirc $^{206}Pb/^{238}U$ date of 87.42+0.78/-0.82 Ma and a concordia intercept date of 86.04±0.84 Ma (Long et al., 2014), which overlaps within error with an 84±2 Ma date obtained by Barton (1987) from a dike sampled from the same drill hole.

Knc Newark Canyon Formation (Lower Cretaceous) Limestone-clast, pebble to cobble conglomerate with red to brown, poorly-sorted, silt- to coarse sand-size matrix; generally matrix-supported, and interbedded with micritic, tan- to light-gray limestone. This unit is only preserved in a series of isolated exposures in the northeast part of the map area; however, the exposure that contains the Knc type-section is present ~1–5 km north of the map area (Nolan et al., 1971; 1974). The type-section is at least 520 m thick (Vandervoort, 1987), has yielded a ~121 Ma (Aptian) maximum deposition age defined by a youngest U-Pb detrital zircon grain population, and a 116.1±1.6 Ma (Aptian) U-Pb crystallization age from a waterlain tuff (Druschke et al., 2010).

Paleozoic Rocks

Pcrc Carbon Ridge Formation, upper conglomerate (Lower Permian) Tan to red weathering, chert-clast pebble conglomerate with a sandy matrix, and dominated by subrounded green and gray chert clasts. Conglomerate is interbedded with medium-bedded, medium-gray, fusilinid-rich limestone, similar to Pcr. Exhibits an interfingering lower contact with Pcr limestone, and forms distinct red to tan soils and slopes. The top of this unit is not exposed in the map area; minimum thickness is 460 m.

Pcr Carbon Ridge Formation (Lower Permian) Tan-weathering, thin-bedded, silty limestone and calcareous siltstone, which outcrops rarely and forms diagnostic tan platy float, and is interbedded with medium-bedded, medium to light-gray, fusilinid-rich limestone, which outcrops more often, and occasionally exhibits dark-brown siliceous stringers and beds. Limestone is interbedded with rare red, non-calcareous siltstone, and rare conglomeratic limestone with chert and fusulinid-bearing clasts. 520 to 640 m thick.

PMe Ely Limestone (Upper Mississippian–Lower Pennsylvanian) Thick- to massive-bedded, blue-gray to medium-gray limestone with abundant diagnostic brown-tan chert nodules and stringers that follow bedding. This unit is absent from the section west of Highway 50, and <30 m is exposed in the northeast part of map area; however, it is up to 460 m thick farther north in the Diamond Mountains (Nolan et al., 1971). These thickness variations are attributed to local deformation and erosion (e.g., Trexler et al., 2004).

Mdp Diamond Peak Formation (Upper Mississippian) Brown- to red-weathering, chert-clast pebble conglomerate, interbedded with tan and red-weathering, coarse-grained sandstone and laminated siltstone, and rare medium-gray sandy limestone. The conglomerate crops out well, and chert clasts are dominantly green and white, and subrounded. 210 to 370 m thick west of Highway 50, and up to 610 m thick in the

eastern part of the map area. Under the stratigraphic divisions of Trexler et al. (2003), the Diamond Peak Formation and the Chainman Shale, regionally, are age-equivalent (Chesterian) rock units, bound at their base by an angular unconformity. Under this interpretation, the underlying black shales mapped here as Chainman Shale may actually be part of the Middle Mississippian Gap Wash Formation (Trexler et al., 2013); see discussion below.

Mc Chainman Shale (Upper Mississippian) ***(possibly equivalent to the Middle Mississippian Gap Wash formation of Trexler et al. [2003])*** Black, thinly-laminated shale interbedded with brown to tan, coarse-grained sandstone and conglomeratic sandstone. Shale rarely outcrops, and weathers into diagnostic black slopes with float chips. Sandstone is more common toward the top of the section, outcrops well, is poorly-sorted and subangular, and has green and dark-gray chert clasts. 550 to 910 m thick. Much or all of this section mapped here as Mc may actually be part of the Middle Mississippian (Meramecian–Osagean) Gap Wash formation (Trexler et al., 2013), originally defined on the Nevada Test Site (Trexler et al., 1996). Under this interpretation, the contact mapped here between Mc and Mdp would represent an angular unconformity (the C2 unconformity of Trexler et al. [2003]), which separates deposits of the Antler foreland basin below from the Antler successor basin above (Trexler et al., 2003).

Mdc Dale Canyon Formation (Mississippian) Interbedded tan, red, and gray siltstone, sandstone, conglomeratic sandstone, local chert pebble conglomerate, and rare black shale. Sandstone is thin- to medium-bedded, poorly-sorted, subangular, lithic rich, and typically tan and red weathering, and is typically light-medium gray when fresh. Coarse sandstone and pebble conglomerate are dominated by green and gray chert clasts. Most lithologies outcrop poorly, and form characteristic platy, tan-red slope-forming float. Weathering rinds are common on siltstone and sandstone float. Sandstone and conglomerate are less mature than Mdp. 270 to 550 m thick.

Mj Joana Limestone (Lower Mississippian) Thin- to medium-bedded, tan- to brown-weathering limestone, interbedded with black shale and siltstone. Limestone is dark-brown to dark-gray when fresh, typically rich in diagnostic crinoid stem fossil hash, and is locally thick-bedded, with brown siliceous stringers. Mj is only exposed in the eastern part of map area. 40 m thick.

MDp Pilot Shale (Upper Devonian–Lower Mississippian) Yellow, olive, and brown-weathering, platy, calcareous, laminated to very thin-bedded black siltstone and shale, interbedded with rare thin-bedded, silty limestone. Not as fissile as Secret Canyon Shale (Cs) or Dunderberg Shale (Cd), and does not outcrop well. Only exposed in the eastern part of the map area. 80 m thick.

DOЄu Devonian, Ordovician, or Cambrian carbonate, undivided Massive, deformed limestone and dolomite of undetermined formation in southern Ratto Canyon; at least 30 m thick.

Ddg Devil's Gate Limestone (Middle–Upper Devonian) Undivided in the Fish Creek and Mountain Boy ranges, where it consists of medium- to thick-bedded, massive-weathering, cliff-forming, medium bluish-gray limestone and lesser interbedded dolomite. Limestone diagnostically weathers like dolomite, forming massive bluffs, exhibits common calcite veining, and exhibits an interfingering lower contact. At least 330 m thick in the Fish Creek Range, and is divided into the following members in the Diamond Mountains:

> **Ddghc Hayes Canyon member** Medium- to blue-gray weathering, medium- to thick-bedded, locally massive-weathering, cliff-forming limestone. Limestone is locally rich in tan, undulatory silty partings that result in platy float, and is very fossiliferous, with crinoids, algal stromatoporoids, and gastropods. Some dark chert near the top. 240–300 m thick.
>
> **Ddgm Meister member** Interbedded dark-bluish-gray, thin-bedded limestone, light-gray, tan, and pink-weathering, thin- to medium-bedded, laminated, creamy dolomite, and less common tan and pink-weathering platy siltstone. 80 m thick.

Nevada Formation (Lower–Middle Devonian)

Divided into the following members in the Diamond Mountains:

> **Dbs Bay State Dolomite member** Massively bedded, medium-gray dolomite, with lesser light-gray and dark-brown dolomite; typically exhibits compositional laminations. Dolomite doesn't alternate colors as regularly as Dsm. Bedding is more apparent and color is typically darker-gray than Slm. Crops out well, and forms cliffy exposures. Mapped in Diamond Mountains only. 180–290 m thick.
>
> **Dw Woodpecker Limestone member** Thin-bedded, dark-gray limestone with common pink-weathering silty partings and interbedded thinly laminated pink to tan siltstone; does not crop out well. Forms diagnostic platy float of dark-gray limestone and pink siltstone. Interbedded with medium- to thick bedded, dark-gray limestone, and massive-weathering dark-gray dolomite. Present in Diamond Mountains, and not present in

Fish Creek and Mountain Boy ranges. 80–120 m thick.

Dsm Sentinel Mountain Dolomite member Alternating gray-brown and light-gray dolomite; meter-scale color alternation is diagnostic. Light-gray dolomite is typically thick-bedded to massive-weathering, and sometimes laminated. Gray-brown dolomite is typically medium- to thick-bedded, commonly laminated, and sometimes mottled. Bedding is well-developed. Both colors of dolomite commonly exhibit diagnostic mottled cm-scale compositional striping. Mapped in Diamond Mountains only. 140–200 m thick.

Doc Oxyoke Canyon Sandstone member Thick-bedded, light-gray, light-brown, and tan-weathering, dolomitic sandstone, with common cross-bedding, and interbedded gray dolomite. Sand is coarse-grained, subangular, moderately-sorted, and dominated by quartz, with muddy matrix. Coarse-grained, white, vitreous, subangular quartzite is locally present, particularly when weathered. Crops out well, and forms diagnostic brown cliffs. Lower and upper contacts are interfingering. 110–150 m thick in the Diamond Mountains.

Dbp Beacon Peak Dolomite member Thin- to medium-bedded, light-gray to white, cream-colored, porcellaneous dolomite, with well-developed bedding. Interbedded with thick-bedded to massive-weathering light-gray to white dolomite, which crops out more commonly. Dolomite is locally rich in tan siliceous stringers, is locally laminated, and exhibits rare spongy tufa-like texture. The white, creamy weathering color is diagnostic. 120–270 m thick.

Dbpq Beacon Peak Dolomite member, basal quartzite Light-gray to white, vitreous, poorly-sorted, massive-weathering quartzite, with medium- to coarse-grained, well-sorted, subangular quartz grains. Quartzite locally weathers light-medium gray and is dolomitic. Forms blocky float, similar to Oe, but Dbpq quartzite is less mature. Commonly brecciated, and crops out well, and bedding planes are more apparent than Oe. Locally present at base of Dbp in the Diamond Mountains, and is not present as a mappable unit in the Fish Creek and Mountain Boy ranges. Up to 30 m thick.

Divided into the following members in the Fish Creek and Mountain Boy ranges:

Ds Simonson Dolostone member Massively-bedded, light-gray, medium-gray, and gray-brown dolomite; generally laminated and mottled. Color alternation between gray and brown dolomite is diagnostic. This unit is mapped in the Fish Creek and Mountain Boy Ranges only, and is laterally-equivalent to the combined Dsm, Dw, and Dbs section mapped in the Diamond Mountains. 430 m thick.

Doc Oxyoke Canyon Sandstone member Same lithology as described above for the Diamond Mountains; however, the percentage by volume of interbedded dolomite is higher in the Fish Creek Range. 110 m thick in the Fish Creek Range.

Dsr Sadler Ranch member Brown to dark-gray, medium- to thick-bedded dolomite with abundant two-hole crinoids, with local interbeds of crinoid-rich limestone. The crinoid-rich packstone and brown color together are diagnostic; fetid odor when broken. Only present in the Fish Creek Range. 90 m thick.

Db Bartine member of the McColley Canyon Formation Medium- to dark-gray, thin- to medium-bedded, platy, fossiliferous limestone. Fossil packstones and wackestones rich in ~1–2 cm shells and crinoids are common. Interbedded with tan- to pink-weathering, thin-bedded, silty limestone and siltstone. Does not outcrop well, and forms platy float-covered slopes. Fetid odor when broken. Only present in the Fish Creek and Mountain Boy ranges. 50–80 m thick.

Dbp Beacon Peak Dolomite member Same lithology as described above for the Diamond Mountains. 50–60 m thick in the Fish Creek Range.

Slm Lone Mountain Dolomite (Silurian) Light-gray, thick-bedded to massive, blocky-weathering, sugary-textured dolomite. Commonly silicified and brecciated, and commonly vuggy. Forms diagnostic light-medium gray slopes and cliffs. At least 400 m thick.

Ohc Hanson Creek Formation (Upper Ordovician) Dark-gray to black, massive-weathering dolomite that is often highly fractured and brecciated, and forms blocky float. Dolomite is interbedded with tan to light green, thin-bedded, micritic, crinoid-bearing limestone higher in the section. At least 50 m thick.

Oe Eureka Quartzite (Middle Ordovician) Vitreous, white, fine-medium grained, well-sorted, sugary quartzite, which commonly weathers gray and red, and is commonly brecciated. Bedding is difficult to recognize without rare

compositional laminations. Rare lags of coarse-grained sandstone and conglomeratic sandstone are present. An interfingering upper contact is observed in the southwest part of map area, but most upper and lower contacts in the map area are structural. Forms distinct white cliffs, and weathers to boulder-size float. 110 m thick.

Opu Pogonip Group undivided (Lower–Middle Ordovician), Divided into the Antelope Valley (Oav), Ninemile (On), and Goodwin (Og) formations described below, except for several areas of alteration that are spatially-associated with the Hoosac fault system. Here, it is mapped as undivided (Opu) where one of the three formations could not be confidently identified as the protolith.

Oav Antelope Valley formation Fossiliferous, thin- to medium-bedded, locally thick-bedded, medium-blue gray, fine-crystalline limestone, with ubiquitous, tan to yellow silty partings. Coiled, cm-scale *maclurites* shells are diagnostic. Limestone exhibits local tan, brown, and white chert nodules, but overall contains much less chert than Og. Exhibits an interfingering lower contact with On. At least 300 m thick.

On Ninemile Formation Platy, thin-bedded, olive-green limey shale and shaly medium-gray limestone, with distinct olive to brown weathering color, and with interbedded silty and sandy limestone. Fossils stand out in relief on bedding planes. Finer-grained lithologies do not crop out well. At least 120 m thick.

Og Goodwin Formation Light- to medium-gray, massive-weathering limestone, and medium-gray, medium- to thick-bedded, silty, well-bedded, fine-crystalline limestone. Light gray, brown, and black chert nodules are common in the lower and upper parts of the section. The middle part of the section is dominated by tan to gray, silty, laminated limestone with silty partings. Limestone outcrops well, exhibits rare intraformational conglomerate, and local fossil hash and lumpy bedding surfaces. The lower contact is placed below the lowest massive limestone; exhibits a gradational upper contact with On. Og limestone is commonly altered to cliffy, massive-weathering cliffs that weather similar to dolomite in the vicinity of Lookout Mountain. At least 350–380 m thick.

Ꞓw Windfall Formation, undivided (Upper Cambrian) Divided into the Bullwhacker member (Ꞓwb) and Catlin member (Ꞓwc) described below, except in Ratto Canyon at the south end of map area. Here, it consists of identical lithologies to Ꞓwb and Ꞓwc, which are interbedded without any clear stratigraphic order, and is mapped as undivided.

Ꞓwb Bullwhacker member Thin-bedded, tan to light-brown, sandy or shaly, medium-gray limestone, with tan-red sandy-shaly partings and interbeds, and diagnostic tan to red weathering color. Trilobite hash and brachiopods are common; exhibits rare gray chert nodules. Does not crop out well; forms characteristic tan-red, platy slope-covering float. 45–80 m thick.

Ꞓwc Catlin member Alternating thick-bedded, massive weathering, medium-coarse crystalline, medium-gray limestone, with common trilobite fossil hash, interbedded with thinner-bedded, sandy-silty limestone with common tan to red, sandy-shaly partings. The massive-weathering limestone outcrops well. Abundant, diagnostic, gray to black, bedded chert is present in the lowest 35 m. Fossil hash weathers out in relief, and wavy and lumpy bedforms are diagnostic. 45–60 m thick.

Ꞓd Dunderberg Shale (Upper Cambrian) Brown, khaki, and gray, fissile, paper-thin, generally non-calcareous shale, with diagnostic, cm-scale nodular limestone discs, and interbeds of medium-bedded, medium-gray limestone. Wavy bedforms commonly form in shale around nodular limestone discs, and limestone interbeds commonly exhibit trilobite fossil hash. Cd shale is more fissile and less silty than Cs. Outcrop-scale folding is common. 45–60 m thick.

Ꞓh Hamburg dolomite (Middle and Upper Cambrian) Massive, light- to medium-gray, coarse-crystalline dolomite, which can exhibit mottled white stringers that define bedding, and white oblong ‘blue bird’ stringers. Dolomite is typically porous or vuggy, and is commonly altered, brecciated, and replaced by jasperoid; extensive collapse brecciation is observed at Lookout Mountain. Ꞓh dolomite is coarser-crystalline, not as well bedded, and lighter gray than Ꞓe dolomite. Exhibits a gradational lower contact, where thin-bedded limestone of Ꞓs alternates with thicker-bedded, crinkly, mottled dark blue limestone of basal Ꞓh, which commonly contains chert stringers. 340–370 m thick.

Ꞓs Secret Canyon Shale (Middle Cambrian) Consists of two distinct interbedded lithologies: 1) thin-bedded, well-bedded, micritic limestone with distinctive mottled yellow or red argillaceous partings, corresponding to the Clarks Spring member of Nolan et al. (1974), and 2) brown, olive, and tan, calcareous, argillaceous shale with local interbedded limestone, corresponding to the shale member of Nolan et al. (1974). The thin-bedded limestone lithology outcrops rarely, and forms diagnostic platy yellow float. The limestone lithology is very fine-grained,

bioturbated, silty, tan to blue-gray when fresh, and with yellow partings yields a highly-banded or mottled appearance. The shale lithology rarely outcrops, and is siltier and not as fissile as Cd shale. Outcrop-scale folding is common. At least 210 m thick; apparent thicknesses up to 400 m may be due in part to structural thickening by outcrop-scale folding.

Cg Geddes Limestone (Middle Cambrian) Well-bedded, thin- to medium-bedded, dark-blue to black, carbonaceous limestone, with maroon-weathering silty and shaly partings, and local black nodular chert. Forms angular, blocky float, and exhibits an interfingering lower contact. Outcrop-scale folding is common, and black color and well-developed bedding is diagnostic. 80–110 m thick.

Ce Eldorado dolomite (Middle Cambrian) Medium-dark gray, massive-weathering dolomite, commonly mottled and streaked with white stringers and spots, giving a speckled ('blue bird') appearance. Dark dolomite locally alternates with lighter-gray, rough-textured dolomite, and can give the appearance of alternating light and dark bands on the order of ~1 foot thick, which defines bedding. Fenestral (bird's eye) structure is common, and light-gray, coarse-crystalline (sanded), massive, featureless dolomite is a common alteration product. Ce dolomite is finer-crystalline, darker gray, and has more apparent bedding than Ch dolomite. The upper contact with Cg limestone is interfingering, and the contact is placed at the highest occurrence of dolomite. Dolomite outcrops well and forms distinct gray cliffs. 560–690 m thick.

Cp Pioche Shale (Lower Cambrian) Khaki to green, and less commonly red-orange, sandy, micaceous, locally calcareous shale. The unit contains thin interbeds of red-brown micaceous sandstone and quartzite similar to Cpm, thin interbeds of mottled, well-bedded, dark-blue limestone with abundant trilobite fragments, and also one ~6 m thick interbed of light-gray weathering dolomite near the top of Prospect Mountain that resembles Ce dolomite. 60–80 m thick.

Cpm Prospect Mountain Quartzite (Lower Cambrian) Well-sorted quartzite that is light tan to white on fresh surfaces, and white, pink, tan, and brown when weathered; exhibits common cross-lamination, and rare pebble conglomerate interbeds. Micaceous to sandy shale interbeds (centimeters to meters thick) are more common in the lower part of the section. Quartzite weathers into angular, pink-brown blocky float, in contrast to Oe, which forms brilliant white cobbles and boulders. At least 550 m thick (base is not exposed).

REFERENCES

Allmendinger, R.W., 1992, Fold and thrust tectonics of the western United States exclusive of the accreted terranes, *in* Burchfiel, B. C., and others, editors, The Cordilleran Orogen—conterminous U.S.: Boulder, Colorado, Geological Society of America, Geology of North America, v. G-3, p. 583–607.

Arehart, G.B., Chakurian, A.M., Tretbar, D.R., Christensen, J.N., McInnes, B.A., and Donelick, R.A., 2003, Evaluation of radioisotope dating of Carlin-type deposits in the Great Basin, western North America, and implications for deposit genesis: Economic Geology, v. 98, p. 235–248.

Armstrong, R.L., 1968, Sevier orogenic belt in Nevada and Utah: Geological Society of America Bulletin, v. 79, p. 429–458.

Armstrong, R.L., 1972, Low-angle (denudation) faults, hinterland of the Sevier orogenic belt, eastern Nevada and western Utah: Geological Society of America Bulletin, v. 83, p. 1729–1754.

Armstrong, R.L., and Ward, P., 1991, Evolving geographic patterns of Cenozoic magmatism in the North American Cordillera—the temporal and spatial association of magmatism and metamorphic core complexes: Journal of Geophysical Research, v. 96, p. 13,201–13,224.

Barnes, C.G., Burton, B.R., Burling, T.C., Wright, J.E., and Karlsson, H.R., 2001, Petrology and geochemistry of the late Eocene Harrison Pass pluton, Ruby Mountains core complex, northeastern Nevada: Journal of Petrology, v. 42, p. 901–929.

Barton, M.D., 1982, Some aspects of the geology and mineralogy of the fluorine-rich skarn at McCullough Butte, Eureka County, Nevada: Carnegie Institution of Washington Year Book, v. 81, p. 324–328.

Barton, M.D., 1987, Lithophile-element mineralization associated with Late Cretaceous two-mica granites in the Great Basin: Geology, v. 15, p. 337–340.

Bentz, M.G., 1983, Progressive structural and stratigraphic events affecting the Roberts Mountains allochthon in the Devil's Gate area, Nevada: Athens, Ohio University, M.S. thesis, 3 plates, scale 1:9600, 222 p.

Best, M.G., and Christiansen, E.H., 1991, Limited extension during peak Tertiary volcanism, Great Basin of Nevada and Utah: Journal of Geophysical Research, v. 96, p. 13,509–13,528.

Best, M.G., Barr, D.L., Christiansen, E.H., Gromme, S., Deino, A.L., and Tingey, D.G., 2009, The Great Basin Altiplano during the middle Cenozoic ignimbrite flareup—insights from volcanic rocks: International Geology Review, v. 51, p. 589–633, doi: 10.1080/00206810902867690.

Best, M.G., Gromme, S., Deino, A.L., Christiansen, E.H., Hart, G.L., and Tingey, D.G., 2013, The 36–18 Ma central Nevada ignimbrite field and calderas, Great Basin, USA—multicyclic super-eruptions: Geosphere, v. 9, p. 1562–1636.

Blake, M.C., McKee, E.H., Marvin, R.F., Silberman, M.L., and Nolan, T.B., 1975, The Oligocene volcanic center at Eureka, Nevada: U.S. Geological Survey Journal of Research, v. 3, p. 605–612.

Brokaw, A.L., Bauer, H.L., and Breitrick, R.A., 1973, Geologic map of the Ruth quadrangle, White Pine County, Nevada: U.S. Geological Survey Geologic Quadrangle Map GQ-1085, scale 1:24 000.

Brew, D.A., 1961a, Lithologic character of the Diamond Peak Formation (Mississippian) at the type locality, Eureka and White Pine counties, Nevada: U.S. Geological Survey Professional Paper 424-C, p. C110–112.

Brew, D.A., 1961b, Relation of Chainman Shale to Bold Bluff thrust fault, southern Diamond Mountains, Eureka and White Pine counties, Nevada: U.S. Geological Survey Professional Paper 424-C, p. C113–C115.

Brew, D.A., 1971, Mississippian stratigraphy of the Diamond Peak area, Eureka County, Nevada, with a section on the biostratigraphy and age of the Carboniferous formations, by Mackenzie Gordon, Jr.: U.S. Geological Survey Professional Paper 661, 84 p.

Burchfiel, B.C., and Davis, G.A., 1975, Nature and controls of Cordilleran orogenesis, western United States—Extension of an earlier synthesis: American Journal of Science, v. 275A, p. 363–396.

Carpenter, D.G., Carpenter, J.A., Dobbs, S.W., and Stuart, C.K., 1993, Regional structural synthesis of Eureka fold-and-thrust belt, east-central Nevada: *in* Gillespie, C.W., editor, Structural and stratigraphic relationships of Devonian reservoir rocks, east-central Nevada: Nevada Petroleum Society 1993 Field Conference Guidebook, p. 59–72.

Cline, J.S., Hofstra, A.H., Muntean, J.L., Tosdal, R.M., and Hickey, K.A., 2005, Carlin-type gold deposits in Nevada—critical geologic characteristics and viable models: Economic Geology, One Hundredth Anniversary Volume, p. 451–484.

Colgan, J.P., and Henry, C.D., 2009, Rapid middle Miocene collapse of the Sevier orogenic plateau in north-central Nevada: International Geology Review, v. 51, p. 920–961.

Colgan, J.P., Henry, C.D., and John, D.A., 2011, Geologic map of the Caetano caldera, Lander and Eureka counties, Nevada: Nevada Bureau of Mines and Geology Map 174, scale 1:75,000, 10 p.

Colgan, J.P., Howard, K.A., Fleck, R.J., Wooden, J.L., 2010, Rapid middle Miocene extension and unroofing of the southern Ruby Mountains, Nevada: Tectonics, v. 29, TC6022, doi:10.1029/2009TC002655.

Cook, H.E., and Corboy, J.E., 2004, Great Basin Paleozoic carbonate platform—facies, facies transitions, depositional models, platform architecture, sequence stratigraphy, and predictive mineral host models: U.S. Geological Survey Open-File Report 2004-1078, 129 p.

Couch, B.F. and Carpenter, J.A., 1943, Nevada's metal and mineral production (1859–1940, inclusive): Nevada Bureau of Mines and Geology Bulletin 38, 159 p.

Cousens, B., Prytulak, J., Henry, C., Alcazar, A., and Brownrigg, T., 2008, Geology, geochronology, and geochemistry of the Miocene–Pliocene ancestral Cascades arc, northern Sierra Nevada, California and Nevada—the roles of the upper mantle, subducting slab, and the Sierra Nevada lithosphere: Geosphere, v. 4., no. 5, p. 829–853.

Crafford, A.E.J., 2007, Geologic map of Nevada, U.S. Geological Survey Data Series 249, 46 p.

Curtis, J.S., 1884, Silver-lead deposits of Eureka, Nevada: U.S. Geological Survey Monograph 7, 200 p.

DeCelles, P.G., 2004, Late Jurassic to Eocene evolution of the Cordilleran thrust belt and foreland basin system, western U.S.A.: American Journal of Science, v. 304, p. 105–168, doi: 10.2475/ajs.304.2.105.

Dickinson, W.R., 1977, Paleozoic plate tectonics and the evolution of the Cordilleran continental margin, *in* Stewart, J.H., Stevens, C.H., and Fritsche, A.E., editors, Paleozoic paleogeography of the western United States, Volume 1: Los Angeles, Pacific Section, Society of Economic Paleontologists and Mineralogists, p. 137–156.

Dickinson, W.R., 2002, The Basin and Range Province as a composite extensional domain: International Geology Review, v. 44, p. 1–38.

Dickinson, W.R., 2006, Geotectonic evolution of the Great Basin: Geosphere, v. 2, p. 353–368, doi:10.1130/GES00054.1.

Dilles, P.A., Wright, W.A., Monteleone, S.E., Russell, K.D., Marlowe, K.E., Wood, R.A., and Margolis, J., 1996, The geology of the West Archimedes deposit: a new gold discovery in the Eureka mining district, Eureka County, Nevada, *in* Coyner, A.R., and Fahey, P.L., editors, Geology and ore deposits of the American Cordillera: Geological Society of Nevada Symposium Proceedings, Reno/Sparks, Nevada, April 1995, p. 159–171.

Drake, E.A., 1978, Paleozoic stratigraphy of the Devil's Gate-northern Mahogany Hills area, Eureka County, Nevada: Oregon State University, M.S. thesis, 6 plates, scale 1:24,000, 110p.

Druschke, P., Hanson, A.D., Wells, M.L., Gehrels, G.E., and Stockli, D., 2010, Paleogeographic isolation of the Cretaceous to Eocene Sevier hinterland, east-central Nevada—insights from U-Pb and (U-Th)/He detrital zircon ages of hinterland strata: Geological Society of

America Bulletin, v. 123, p. 1141–1160, doi: 10.1130/B30029.1.

Frost, B.R., Arculus, R.J., Barnes, C.G., Collins, W.J., Ellis, D.J., and Frost, C.D., 2001, A geochemical classification of granitic rocks: Journal of Petrology, v. 42, p. 2033–2048.

Gans, P.B., and Miller, E.L., 1983, Style of mid-Tertiary extension in east-central Nevada: Utah Geological and Mineral Survey Special Studies 59, p. 107–160.

Gans, P.B., Seedorff, E., Fahey, P.L., Hasler, R.W., Maher, D.J., Jeanne, R.A., and Shaver, S.A., 2001, Rapid Eocene extension in the Robinson district, White Pine County, Nevada—constraints from $^{40}AR/^{39}AR$ dating: Geology, v. 29, p. 475–478.

Gromme C.S., McKee E.H., and Blake M.C., Jr., 1972, Paleomagnetic correlations and potassium-argon dating of middle Cenozoic ash-flow sheets in the eastern Great Basin, Nevada and Utah: Geological Society of America Bulletin, v. 83, p. 1619–1638.

Gustin, M. M., 2013, Updated technical report on the Lookout Mountain project Eureka County, Nevada, USA, prepared for Timberline Resources Corp. 142 p.

Hague, A., 1892, Geology of the Eureka district, Nevada: U.S. Geological Survey Monograph 20, 419 p.

Hastings, M.H., 2008, Relationship of base-metal skarn mineralization to Carlin-type gold mineralization at the Archimedes gold deposit, Eureka, Nevada: University of Nevada, Reno, M.S. thesis, 109 p.

Henry, C.D., 2008, Ash-flow tuffs and paleovalleys in northeastern Nevada—implications for Eocene paleogeography and extension in the Sevier hinterland, northern Great Basin: Geosphere, v. 4, p. 1–35.

Henry, C.D., and John, D.A., 2013, Magmatism, ash-flow tuffs, and calderas of the ignimbrite flareup in the western Nevada volcanic field, Great Basin, USA: Geosphere, v. 9, p. 951–1008.

Henry, C.D., and Ressel, M.W., 2000, Interrelation of Eocene magmatism, extension, and Carlin-type gold deposits in northeastern Nevada, *in* Lageson, D.R., Peters, S.G., and Lahren, M.M., editors, Great Basin and Sierra Nevada: Boulder, Colorado, Geological Society of America Field Guide 2, p. 165–187.

Hofstra, A.H., and Cline, J.S., 2000, Characteristics and models for Carlin-type gold deposits: Reviews in Economic Geology, v. 13, p. 163–220.

Hofstra, A.H., Snee, L.W., Rye, R.O., Folger, H.W., Phinisey, J.D., Loranger, R.J., Dahl, A.R., Naesar, C.W., Stein, H.J., and Lewchuk, 1999, Age constraints on Jerritt Canyon and other Carlin-type gold deposits in the western United States—relationship to mid-Tertiary extension and magmatism: Economic Geology, v. 94, p. 769–802.

Hollabaugh, C.L., and Purcell, V.L., 1987, Garnet Hill, White Pine County, Nevada: Mineralogical Record, v. 18, p. 195–198.

Humphreys, E.D., 1995, Post-Laramide removal of the Farallon slab, western United States: Geology, v. 23, p. 987–990.

John, D.A., Henry, C.D., and Colgan, J.P., 2008, Magmatic and tectonic evolution of the Caetano caldera, north-central Nevada—a tilted, mid-Tertiary eruptive center and source of the Caetano Tuff: Geosphere, v. 4, p. 75–106.

John, D.A., Colgan, J.P., Henry, C.D., Wooden, J.L., 2009, Prolonged Eocene magmatism culminating with the Caetano caldera, Cortez area, Nevada—inferences from SHRIMP U-Pb zircon dating: Eos Transactions, American Geophysical Union, v. 90, no. 52, V41B-2187.

Kistler, R.W., Ghent, E.D., and O'Neill, J.R., 1981, Petrogenesis of garnet two-mica granites in the Ruby Mountains, Nevada: Journal of Geophysical Research, v. 86, p. 10,591–10,606

Kuiper, K.F., Deino, A., Hilgen, F.J., Krijgsman, W., Renne, P.R., and Wijbrans, J.R., 2008, Synchronizing rock clocks of Earth history: Science, v. 320, p. 500–504.

Lisenbee, A.L., 2001, Structure and stratigraphy of the Eureka area, *in* Miller, M.S., and Walker, J.P., editors, Structure and stratigraphy of the Eureka, Nevada, area: Reno, Nevada Petroleum Society 2001 Fieldtrip Guidebook, p. 43–58.

Lisenbee, A.L., Monteleone, S.R., and Saucier, A.E., 1995, The Hoosac thrust and related faults, Eureka region, Nevada: *in* Hansen, M.W., Walker, J.W., and Trexler, J.H., editors, Mississippian source rocks in the Antler basin of Nevada and associated structural and stratigraphic traps: Nevada Petroleum Society 1995 Fieldtrip Guidebook, p. 115–121.

Long, S.P., 2012, Magnitudes and spatial patterns of erosional exhumation in the Sevier hinterland, eastern Nevada and western Utah, U.S.A.—insights from a Paleogene paleogeologic map: Geosphere, v. 8, p. 881–901, doi: 10.1130/GES00783.1.

Long, S.P., Henry, C.D., Muntean, J.L., Edmondo, G.P., and Cassel, E.J., 2014, Early Cretaceous construction of a structural culmination, Eureka, Nevada, U.S.A.: implications for out-of-sequence deformation in the Sevier hinterland: Geosphere, v. 10, 21 p., doi: 10.1130/GES00997.1.

Long, S.P., Henry, C.D., Muntean, J.L., Edmondo, G.P., and Cassel, E.J., 2014, Early Cretaceous construction of a structural culmination, Eureka, Nevada, U.S.A.: implications for out-of-sequence deformation in the Sevier hinterland: Geosphere, v. 10, p. 564–584, doi:10.1130/GES00997.1.

Ludwig, K.R., 2008, Isoplot 3.70, A geochronological tool kit for Microsoft Excel: Berkeley Geochronology Center Special Publication no. 4, Berkeley, California.

Ludwig, K.A., and Mundil, R., 2002, Extracting reliable U–Pb ages and errors from complex populations of zircons from Phanerozoic tuffs: Geochemica et Cosmochimica Acta, v. 66, no. 15A, p. 463.

Margolis, J., 1997, Gold paragenesis in intrusion-marginal sediment-hosted gold mineralization at Eureka, Nevada, *in* Vikre, P., Thompson, T.B., Bettles, K., Christensen, O, and Parratt, R., editors, Carlin-type gold deposits field conference: Geological Society of Nevada Guidebook Series 28, p. 213–221.

Marvin, R.F. and Cole, J.C., 1978, Radiometric ages—compilation A, U.S. Geological Survey: Isochron/West, No. 22, p. 3–14.

McIntosh, W.C., Heizler, M., Peters, L., and Esser, R., 2003, $^{40}Ar/^{39}Ar$ geochronology at the New Mexico Bureau of Geology and Mineral Resources: New Mexico Bureau of Geology and Mineral Resources Open-File Report OF-AR-1, 10 p.

Miller, C.F., 1985, Are strongly peraluminous magmas derived from pelitic sedimentary sources: Journal of Geology, v. 93, p. 673–689.

Min, K., Mundil, R., Renne, P.R., and Ludwig, K.R., 2000, A test for systematic errors in $^{40}Ar/^{39}Ar$ geochronology through comparison with U/Pb analysis of a 1.1 Ga rhyolite: Geochimica et Cosmochimica Acta, v. 64, p. 73–98.

Mortensen, J.K., Thompson, J.F.H., and Tosdal, R.M., 2000, U-Pb age constraints on magmatism and mineralization in the northern Great Basin, Nevada, *in* Cluer, J.K., Price, J.G., Struhsacker, E.M., Hardyman, R.F., and Morris, C.L., editors, Geology and ore deposits 2000—the Great Basin and beyond: Geological Society of Nevada Symposium Proceedings, May 15–18, p. 419–438.

Muntean, J.L., 2009, Major precious metal deposits, *in* Price, J.G., Muntean, J.L., Davis, D.A., Hess, R.H., and Shevenell, L., The Nevada mineral industry 2008: Nevada Bureau of Mines and Geology Special Publication MI-2008, p. 84–114.

Muntean, J.L., Cline, J.S., Simon, A.C., and Longo, A.A., 2011, Magmatic-hydrothermal origin of Nevada's Carlin-type gold deposits: Nature Geoscience, v. 4, p. 122–127.

Nevada Bureau of Mines and Geology, 2014, The Nevada Mineral Industry 2012: Nevada Bureau of Mines and Geology Special Publication MI-2012, 177 p.

Nolan, T.B., 1962, The Eureka mining district, Nevada: U.S. Geological Survey Professional Paper 406, 78 p.

Nolan, T.B., and Hunt, R.N., 1968, The Eureka mining district, Nevada, *in* Ore deposits of the United States (Graton-Sales Volume), v. 1, p. 966–991.

Nolan, T.B., Merriam, C.W., and Williams, J.S., 1956, The stratigraphic section in the vicinity of Eureka, Nevada: U.S. Geological Survey Professional Paper 276, 77 p.

Nolan, T.B., Merriam, C.W., and Brew, D.A., 1971, Geologic map of the Eureka quadrangle, Eureka and White Pine counties, Nevada: U.S. Geological Survey Miscellaneous Investigations Series, Map I-612: 1:31,680-scale, 8 p., 2 plates.

Nolan, T.B., Merriam, C.W., and Blake, M.C., Jr., 1974, Geologic map of the Pinto Summit quadrangle, Eureka and White Pine counties, Nevada: U.S. Geological Survey Miscellaneous Investigations Series, Map I-793: 1:31,680-scale, 14 p., 2 plates.

Oldow, J.S., 1984, Evolution of a late Mesozoic back-arc fold and thrust belt, northwestern Great Basin, U.S.A.: Tectonophysics, v. 102, p. 245–274, doi: 10.1016/0040-1951(84)90016-7.

Pabst, Adolf, 1938, Garnets from vesicles in rhyolite near Ely, Nevada: American Mineralogist, v. 23, p. 101–103.

Palmer, A.R., 1960, Identification of the Dunderberg shale of Late Cambrian age in the eastern Great Basin: U.S. Geological Survey Professional Paper 400-B, p. B289–B290.

Pearce, J. A. and Peate, D.W., 1995, Tectonic implications of the composition of volcanic arc magmas, Annual Review of Earth and Planetary Sciences, 23, p. 251–285.

Poole, F.G., 1974, Flysch deposits of Antler foreland basin, western United States, *in* Dickinson, W.R., ed., Tectonics and sedimentation: Society of Economic Paleontologists and Mineralogists Special Publication 22, p. 58–82.

Poole, F.G., and Sandberg, C.A., 1977, Mississippian paleogeography and tectonics of the western United States, *in* Stewart, J.H., Stevens, C.H., and Fritsche, A.E., editors, Paleozoic paleogeography of the western United States: Los Angeles, Society of Economic Paleontologists and Mineralogists, Pacific Section, p. 67–85.

Ransom, K.L., and Hansen, J.B., 1993, Cretaceous transpressional deformation, Eureka County, Nevada: *in* Gillespie, C. W., editor, Structural and stratigraphic relationships of Devonian reservoir rocks, east-central Nevada: Nevada Petroleum Society 1993 Field Conference Guidebook, p. 89–104.

Ressel, M.W., and Henry, C.D., 2006, Igneous geology of the Carlin trend, Nevada: Development of the Eocene plutonic complex and significance for Carlin-type gold deposits: Economic Geology, v. 101, p. 347–383.

Rich, M., 1977, Pennsylvanian paleogeographic patterns in the western United States, *in* Stewart, J.H., Stevens, C.H., and Fritsche, A.E., editors, Paleozoic paleogeography of the western United States: Society of Economic Paleontologists and Mineralogists, Pacific Section, Pacific Coast Paleogeography Symposium 1, p. 87–111.

Ross, R.J., Jr., 1970, Ordovician brachiopods, trilobites, and stratigraphy in eastern and central Nevada: U.S. Geological Survey Professional Paper 639, 103 p.

Russel, K.D., 2000, Influence of structure on ore occurrence, Archimedes gold deposit, Eureka County, Nevada, *in* Cluer, J.M., Price, J.G., Struhsacker, E.M., Hardyman, R.T., and Morris, C.L., editors, Geology and Ore Deposits 2000: The Great Basin and Beyond: Geological Society of Nevada Symposium Proceedings, 2000, Reno/Sparks, NV, v. 1, p. A13.

Ryskamp, E.R., Abbott, J.T., Christiansen, E.H., Keith, J.D., Vervoort, J.D., and Tingey, D.V., 2008, Age and petrogenesis of volcanic and intrusive rocks in the Sulphur Spring Range, central Nevada: Comparisons with ore-associated Eocene magma systems in the Great Basin: Geosphere, v. 4, p. 496–519.

Samson, S.D. and Alexander, E.C., Jr., 1987, Calibration of the interlaboratory $^{40}Ar/^{39}Ar$ dating standard, MMhb-1: Chemical Geology, v. 66, p. 27–34.

Smith, J.F., Jr., and Ketner, K.B., 1977, Tectonic events since early Paleozoic in the Carlin–Pinon Range area, Nevada: U.S. Geological Survey Professional Paper 876C, 18 p.

Smith, R.M., 1976, Geology and mineral resources of White Pine County, Nevada, part II—mineral resources, p. 36–105, *in* Hose, R.K., Blake, M.C., Jr., and Smith, R.M., Geology and mineral resources of White Pine County, Nevada: Nevada Bureau of Mines and Geology Bulletin 85, 105 p., scale 1:250,000.

Speed, R.C., and Sleep, N., 1982, Antler orogeny and foreland basin: A model: Geological Society of America Bulletin, v. 93, p. 815–828.

Steiger, R.H., and Jäger, E., 1977, Subcommission on geochronology: Convention on the use of decay constants in geo- and cosmochronology: Earth and Planetary Science Letters, v. 36, p. 359–362.

Steininger, R.C., Klessig, P.J., Young, T.H., 1987, Geology of the Ratto Canyon gold deposits, Eureka County, Nevada, *in* Johnson, J.L., editor, Bulk mineable precious metal deposits of the western United States, Guidebook for Field Trips: Geological Society of Nevada, Reno, p. 293–304.

Stewart, J.H., 1962, Variable facies of the Chainman and Diamond Peak Formations in western White Pine County, Nevada: U.S. Geological Survey Professional Paper 450-C, p. C57–C60.

Stewart, J.H., and Poole, F.G., 1974, Lower Paleozoic and uppermost Precambrian Cordilleran miogeocline, Great Basin, western United States, *in* Dickinson, W.R., editor, Tectonics and Sedimentation: Society of Economic Paleontologists and Mineralogists Special Publication 22, p. 28–57.

Taylor, W.J., Bartley, J.M., Fryxell, J.E., Schmitt, J., and Vandervoort, D.S., 1993, Mesozoic Central Nevada thrust belt, *in* Lahren, M.M., Trexler, J.H., and Spinosa, C., editors, Crustal Evolution of the Great Basin and the Sierra Nevada: Geological Society of America Cordilleran/Rocky Mountain Sections Field Trip Guidebook: Boulder, p. 57–96.

Taylor, W.J., Bartley, J.M., Martin, M.W, Geissman, J.W., Walker, J.D., Armstrong, P.A., and Fryxell, J.E., 2000, Relations between hinterland and foreland shortening: Sevier orogeny, central North American Cordillera: Tectonics, v. 19, no. 6, p. 1124–1143.

Tosdal, R.M., Wooden, J.L., and Kistler, R.W., 2000, Geometry of the Neoproterozoic continental breakup, and implications for location of Nevadan mineral belts, *in* Cluer, J.K., Price, J.G., Struhsacker, E.M., Hardyman, R.F., and Morris, C.L., editors, Geology and Ore Deposits 2000, The Great Basin and Beyond, Symposium Proceedings, Geological Society of Nevada, Reno, p. 451–466.

Trexler, J.H., Cole, J.C., and Cashman, P.H., 1996, Middle Devonian–Missippian stratigraphy on and near the Nevada Test Site: implications for hydrocarbon potential: American Association of Petroleum Geologists Bulletin, v. 80, p. 1736–1762.

Trexler, J.H., Cashman, P.H., Cole, J.C., Snyder, W.S., Tosdal, R.M., and Davydov, V.I., 2003, Widespread effects of middle Mississippian deformation in the Great Basin of western North America: Geological Society of America Bulletin, v. 115, p. 1278–1288, doi: 10.1130/B25176.1.

Trexler, J.H., Cashman, P.H., Snyder, W.S., and Davydov, V.I., 2004, Late Paleozoic tectonism in Nevada: timing, kinematics, and tectonic significance: Geological Society of America Bulletin, v. 116, p. 525-538, doi: 10.1130/B25295.1.

Trexler, J.H., Cashman, P., French, D., and Walker, J.D., 2013, The underappreciated Middle Mississippian (C2) unconformity in the Great Basin—its tectonic and stratigraphic significance (absract): Rocky Mountain Section, American Association of Petroleum Geologists Section meeting, Salt Lake City, p. 70.

U.S. Geological Survey and Nevada Bureau of Mines and Geology, 2006, Quaternary fault and fold database for the United States, accessed June 21, 2012, from USGS website: http//earthquake.usgs.gov/regional/qfaults/

Vandervoort, D.S., 1987, Sedimentology, provenance, and tectonic implications of the Cretaceous Newark Canyon Formation, east-central Nevada: Bozeman, Montana State University, M.S. thesis, 145 p.

Vikre, P.G., 1998, Intrusion-related, polymetallic carbonate replacement deposits in the Eureka district, Eureka County, Nevada: Nevada Bureau of Mines and Geology Bulletin 110, 52 p.

Walcott, C.D., 1884, The paleontology of the Eureka district, Nevada: U.S. Geological Survey Monograph 8, 298 p.

Westra, G., and Riedell, K.B., 1996, Geology of the Mount Hope stockwork molybdenum deposit, Eureka County, Nevada, *in* Coyner, A.R., and Fahey, P.L., eds., Geology and ore deposits of the American Cordillera: Geological Society of Nevada Symposium Proceedings, Reno/Sparks, Nevada, p. 1639–1666.

Whalen, J.B., Currie, K.L. & Chappell, B.W., 1987, A-type granites—geochemical characteristics, discrimination and petrogenesis: Contributions to Mineralogy and Petrology, v. 95, p. 407–419.

Wilson, W.L., and Wilson, W.B., 1986, Geology of the Eureka-Windfall and Rustler gold deposits, Eureka County, Nevada, *in* Tingley, J.V., and Bonham, H.F., editors, Sediment-hosted precious-metal deposits of northern Nevada: Nevada Bureau of Mines and Geology Report 40, p. 81–84.

Wyld, S.J., 2002, Structural evolution of a Mesozoic backarc fold-and-thrust belt in the U.S. Cordillera—new evidence from northern Nevada: Geological Society of America Bulletin, v.114, p. 1452–1468, doi:10.1130/0016-7606(2002)114<1452:SEOAMB>2.0.CO2;

Suggested Citation:

Long, S.P., Henry, C.D., Muntean, J.L., Edmondo, G.P., and Thomas, R.D., 2014, Geologic map of the southern part of the Eureka mining district and surrounding areas of the Fish Creek Range, Mountain Boy Range, and Diamond Mountains, Eureka and White Pine counties, Nevada: Nevada Bureau of Mines and Geology Map 183, 2 plates, scale 1:24,000, 36p.

Table 3: Chemical analyses of igneous rocks of the Eureka area, Eureka County, Nevada

Sample Number	Rock	Location	Strat	vit_devit	Unit	garnet	Age28201	error	Lat27	Long27	Lab	SiO_2	TiO_2	$Al2O_3$	FeO	MnO	MgO	CaO	Na_2O	K_2O	P_2O_5	LOI	Total	FeO/(FeO+MgO)	Na_2O+K_2O	Alum2	V	Cr	Co	Ni	Cu	Zn	Ga	Rb	Sr	Y	Zr	Nb	Mo	Ag	Sn	Cs	Ba	Hf	Ta	W	Tl	Pb	Th	U	La	Ce	Pr	Nd	Sm	Eu	Gd	Tb	Dy	Ho	Er	Tm	Yb	Lu
H12-86	Magpie Hill Basalt lava	Rescue Canyon			Tmh	No			39.38948	-115.88248	ALS ICP-OES, MS	52.41	2.43	15.87	10.17	0.18	4.14	7.03	4.42	2.45	0.8	0.10	101.65	0.544	6.87	0.730	163	100	31.8	47	16	120	21.7	59.1	823.2	31.4	333.5	66.8	3	<1	2	0.45	805	7.9	4.3	<1	<0.5	<5	6.31571883	1.6	49.2	99.4	11.71	45.9	9.28	2.64	7.82	1.12	6.25	1.21	3.28	0.45	2.82	0.44
H12-85	Pancake Summit Tuff	Rescue Canyon			Tps	No			39.40916	-115.86711	ALS ICP-OES, MS	75.55	0.15	13.01	1.53	0.06	0.49	1.28	3.12	4.76	0.02	3.61	99.08	0.307	7.88	1.033	9	10	1.6	8	<5	45	22.6	239.8	66.5	40.7	101.8	39.1	6	<1	2	25.71	153	5.5	4.3	5	1.7	31	45.436575	13.6	25.4	51.4	7.31	28.5	7.2	0.28	6.54	1.07	6.79	1.33	4.53	0.67	4.44	0.72
H11-77	aphyric andesite lava	northeast map area			Trma	No		35.67	0.16	39.46217	-115.86688	ALS ICP-OES, MS	59.92	0.68	14.96	6.33	0.11	4.95	7.09	2.18	3.53	0.25	0.40	98.62	0.561	5.71	0.748	161	152	25.1	23	17	85	19.4	121	515	21.6	163	15.8	2	<1	2	3.66	1080	4.5	1.2	1	0.5	16	13.13	3.53	39.4	70.7	8.02	30.6	6.24	1.3	4.5	0.65	3.96	0.76	2.19	0.31	2	0.3
H11-78	aphyric andesite lava	northeast map area			Trma	No		39.46459		39.46459	-115.88142	ALS ICP-OES, MS	60.15	0.65	14.71	6.44	0.12	4.92	7.15	2.24	3.4	0.21	0.60	99.59	0.567	5.64	0.731	157	181	24.9	25	15	82	18.9	123	481	21.5	154	15.6	2	<1	2	4.55	998	4.4	1.2	1	0.5	16	12.55	3.6	37.5	66.6	7.56	28.7	5.9	1.23	4.43	0.62	3.81	0.72	2.12	0.3	1.98	0.3
H11-102	aphyric andesite dike	S of Richmond Mountain			Trma	No		36.2		39.48929	-115.91609	ALS ICP-OES, MS	60.6	0.67	14.87	6.23	0.1	4.43	7.09	2.3	3.45	0.26	1.10	99.17	0.584	5.75	0.740	161	182	25	25	17	86	19.6	133	496	22.6	160	15.9	<2	<1	2	3.93	1039	4.4	1.2	1	0.5	15	12.6	3.71	38.5	68.5	7.91	30.3	6.28	1.33	4.61	0.66	3.99	0.77	2.13	0.32	2.06	0.32
H11-103	aphyric andesite dike	S of Richmond Mountain			Trma	No		36.2		39.49089	-115.91726	ALS ICP-OES, MS	59.78	0.76	16.5	6.63	0.11	3.6	6.47	2.25	3.58	0.31	0.80	96.35	0.648	5.83	0.870	167	93	24.7	17	15	105	22.8	146	674	22	236	16.9	2	<1	2	3.85	1417	6.1	1	1	0.5	15	18.53	3.08	61.5	106.9	11.73	44.1	8.02	1.65	5.55	0.71	4.09	0.79	2.16	0.3	2.08	0.3
H11-105	aphyric andesite lava	top of Richmond Mountain			Trma	No		36.2		39.49972	-115.92779	ALS ICP-OES, MS	60.97	0.96	15.6	6.42	0.11	3.48	6.02	2.42	3.71	0.33	1.50	98.41	0.648	6.13	0.841	131	102	17.4	8	7	91	21.2	127	669	23.4	233	19.5	2	<1	2	2.16	1184	5.9	1.1	1	<0.5	13	13.52	2.61	57.8	100.4	11.58	43.6	8.21	1.71	5.84	0.73	4.42	0.81	2.29	0.3	2	0.3
H11-106	aphyric andesite lava, sparse hornblende	top of Richmond Mountain			Trma	No		36.2		39.49923	-115.92696	ALS ICP-OES, MS	61.41	0.68	15.35	6.09	0.11	3.68	6.11	2.5	3.78	0.28	0.00	98.03	0.623	6.28	0.809	129	102	19.9	17	13	90	21.2	147	593	17.9	236	16.3	2	<1	2	3.67	1367	6.1	1	1	0.5	16	22.65	3.52	67.5	115.3	12.19	44.3	7.46	1.47	4.55	0.59	3.47	0.64	1.73	0.24	1.67	0.26
H11-107	aphyric andesite lava	upper Richmond Mountain			Trma	No		36.16	0.12	39.49920	-115.92598	ALS ICP-OES, MS	61.64	0.68	15.33	6.18	0.1	3.43	6.16	2.41	3.79	0.28	1.30	98.48	0.643	6.2	0.810	126	102	19.2	16	14	92	20.9	151	593	18.9	235	16.3	<2	<1	2	4.37	1401	6.2	1	1	0.6	16	22.34	3.5	68.1	110.7	12.29	44.6	7.65	1.49	4.82	0.59	3.57	0.65	1.78	0.24	1.71	0.27
H11-90	plag-biotite-hornblende dacite	Ratto Canyon			Trmv	No		36.16	0.07	39.40238	-115.99060	ALS ICP-OES, MS	68.39	0.53	15.94	3.54	0.07	1.01	3.41	3.12	3.78	0.2	2.89	97.24	0.778	6.9	1.050	36	10	4.9	<5	<5	93	22.9	133	643	17.4	260	22.2	3	<1	2	2.24	1378	6.7	1.4	1	<0.5	19	19.03	4.11	70.2	114.2	12.29	42.2	7.01	1.46	4.58	0.59	3.25	0.6	1.64	0.25	1.58	0.24
H11-91	plag-biotite dacite	Ratto Canyon			Trmv	No		36.2		39.40301	-115.99113	ALS ICP-OES, MS	70.10	0.46	15.27	3.06	0.06	0.86	3.15	2.78	4.08	0.18	3.50	94.30	0.781	6.86	1.053	35	<10	3.8	<5	<5	78	21.3	116	674	18	240	17.9	2	<1	2	1.65	1803	6.4	1.1	1	0.7	18	21.21	3.26	86.3	142.6	14.85	51.6	8.27	1.72	5.03	0.6	3.47	0.64	1.74	0.24	1.64	0.24
H11-108	plag-pyroxene dacite lava dome	south part of Richmond Mountain			Trmv	No		36.2		39.49779	-115.99203	ALS ICP-OES, MS	64.02	0.88	15.43	5.29	0.05	2.08	4.73	2.93	3.71	0.29	1.10	97.85	0.720	6.64	0.948	101	41	11.8	6	<5	98	22.3	120	652	25.9	257	24.9	2	<1	2	1.93	1360	6.6	1.5	1	<0.5	16	16.71	3.34	63.3	113.4	12.88	47.9	8.94	1.77	5.93	0.81	4.57	0.9	2.48	0.36	2.29	0.35
H11-134	plag-hornblende-pyroxene dacite lava	northwest of Richmond Mountain			Trmv	No		36.2		39.50922	-115.94997	ALS ICP-OES, MS	64.03	0.89	15.35	5.69	0.09	2.10	5.07	2.66	3.82	0.29	2.59	95.12	0.730	6.48	0.883	105	42	12.6	7	<5	97	22.5	122	659	26.2	254	25.3	3	<1	2	2.01	1361	6.9	1.6	1	0.5	17	17.08	3.28	67.5	115.6	13.25	49.4	9.1	1.83	6.44	0.86	5.08	0.95	2.63	0.37	2.5	0.36
H11-65	plag-biotite rhyolite lava dome	South Ratto Canyon			Trl	No		**35.8**		39.37307	-115.98259	ALS ICP-OES, MS	74.93	0.16	13.31	2.08	0.03	0.20	1.16	3.21	4.87	0.05	0.40	99.96	0.912	8.08	1.056	8	10	0.8	<5	<5	50	21.6	203	283	23.3	194	20.3	2	<1	4	3.55	1110	5.7	1.8	1	0.8	27	23.41	4.3	57.2	92.2	11.95	38.9	6.91	1.3	5.7	0.77	4.4	0.82	2.24	0.33	2.04	0.3
H11-62	dacite ash-flow tuff vitrophyre	south Ratto Canyon		vitrophyre	Ttt	No		35.91	0.16	39.37513	-115.97200	ALS ICP-OES, MS	67.85	0.72	14.93	4.57	0.09	1.47	3.76	2.98	3.45	0.18	2.59	98.15	0.757	6.43	0.979	95	10	8.8	<5	<5	85	22.6	116	570	27.9	259	22.8	2	<1	2	2.12	2129	6.9	1.5	1	<0.5	17	18.54	3.48	58.4	112.1	12.79	44.1	7.83	1.82	6.6	0.91	5.33	1.02	2.81	0.42	2.58	0.38
H11-60	dacite ash-flow tuff vitrophyre	south Ratto Canyon			Ttt	No		35.8		39.37624	-115.97467	ALS ICP-OES, MS	68.16	0.72	15.40	4.19	0.05	1.15	3.55	3.25	3.33	0.20	1.59	99.04	0.785	6.58	1.015	87	10	7.7	<5	<5	88	24.1	97	592	28.7	268	24.3	<2	<1	2	1.14	1131	6.7	1.5	1	<0.5	18	18.48	3.04	63	117.1	13.78	46.4	8.35	1.93	6.43	0.87	5.28	1	2.68	0.37	2.39	0.33
H11-59	dacite ash-flow tuff	south Ratto Canyon			Ttt	No		35.83	0.04	39.37615	-115.97514	ALS ICP-OES, MS	69.39	0.64	15.33	3.84	0.06	1.05	3.22	2.96	3.34	0.15	3.18	97.85	0.785	6.3	1.083	74	10	7.6	<5	<5	76	22.7	107	519	27.3	260	23.1	<2	<1	2	2.19	1119	7.2	1.6	1	<0.5	19	21.05	3.6	59.7	113.9	12.98	44.3	7.8	1.81	6.33	0.86	5.24	1.01	2.87	0.42	2.63	0.38
H11-58	dacite ash-flow tuff	south Ratto Canyon			Ttt	No		35.8		39.37826	-115.97538	ALS ICP-OES, MS	67.96	0.70	15.53	4.79	0.07	1.16	3.36	2.79	3.43	0.21	3.40	95.94	0.805	6.22	1.097	84	10	9.5	<5	<5	93	24.9	145	570	28.8	304	24.8	2	<1	2	2.39	975	7.7	1.6	1	<0.5	20	20.48	3.63	64.9	125.1	14.02	47.3	8.2	1.8	6.36	0.85	5.15	0.97	2.72	0.4	2.48	0.36
H11-57	dacite pumice	south Ratto Canyon			Ttp	No		35.8		39.37842	-115.97535	ALS ICP-OES, MS	68.15	0.58	16.80	4.05	0.04	1.24	3.20	2.36	3.42	0.16	7.89	93.18	0.766	5.78	1.272	65	11	5.3	<5	<5	80	24.1	144	497	24.9	248	23.5	2	<1	2	2.43	986	6.8	1.7	1	<0.5	18	22.54	3.96	66.6	114.3	14.11	47.2	7.91	1.72	5.68	0.76	4.56	0.84	2.36	0.34	2.18	0.32
H11-55	rhyolite tuff	south Ratto Canyon			Ttt	No		35.8		39.37899	-115.97516	ALS ICP-OES, MS	76.74	0.05	13.18	1.22	0.05	0.36	1.00	2.65	4.74	0.01	4.19	94.86	0.772	7.39	1.167	<5	<10	0.6	<5	<5	51	23.6	258	82	33.9	80	32	2	<1	7	7.05	236	3.7	4.4	2	0.8	34	23.4	9.97	14.8	27.4	3.77	13.7	4.22	0.44	4.72	0.84	5.66	1.12	3.23	0.5	3.18	0.45
H11-61	dacite ash-flow tuff	south Ratto Canyon		vitrophyre	Ttt	No		35.8		39.37875	-115.97710	ALS ICP-OES, MS	68.32	0.71	15.30	4.39	0.06	1.17	3.47	3.02	3.39	0.17	2.50	98.06	0.790	6.41	1.038	87	10	7.8	<5	<5	85	23.9	120	559	28.3	269	23.8	2	<1	2	2.04	1071	6.8	1.5	1	<0.5	18	19.38	3.34	60.9	112.2	13.21	45.8	8.16	1.9	6.56	0.9	5.26	1	2.69	0.39	2.44	0.35
H11-64	dacite ash-flow tuff	south Ratto Canyon			Ttt	No		35.77	0.14	39.38298	-115.97474	ALS ICP-OES, MS	68.29	0.72	15.37	4.33	0.06	1.27	3.51	2.96	3.31	0.18	3.39	96.94	0.773	6.27	1.051	89	10	8.1	<5	<5	85	23.8	119	553	28.1	283	23.9	2	<1	2	2.02	1166	7.6	1.7	1	<0.5	19	19.55	3.35	62.4	115	13.67	46.4	8.22	1.97	6.93	0.94	5.56	1.04	2.83	0.41	2.48	0.36
H11-93	dacite ash-flow tuff vitrophyre	Ratto Canyon			Ttt	No		35.8		39.39960	-115.98763	ALS ICP-OES, MS	65.29	0.86	16.56	5.31	0.10	1.86	4.64	2.79	3.35	0.24	2.59	95.73	0.741	6.14	0.951	107	21	11.8	<5	<5	104	23.1	113	658	28.8	269	23.7	<2	<1	2	2.05	1144	7.2	1.5	1	0.6	17	16.92	3.29	68.3	121.7	13.94	52.8	10.88	1.86	6.82	0.9	5.49	1.02	2.8	0.4	2.51	0.4
H11-70	porphyritic rhyolite lava	near Sugarloaf			Trf	No		35.8		39.40234	-115.95324	ALS ICP-OES, MS	77.92	0.09	12.68	1.64	0.03	0.25	0.72	1.62	5.04	0.02	2.89	97.79	0.868	6.66	NM	5	<10	0.7	<5	<5	54	22.4	277	85	27.2	153	33.6	<2	<1	6	6.21	435	5	<1	1	0.9	26	28.33	4.35	32.4	54.8	6.92	23.2	5.05	0.59	4.95	0.75	4.67	0.88	2.51	0.38	2.42	0.35
H11-98	porphyritic rhyolite lava	Ratto Canyon			Ttr	No		35.87		39.39219	-115.98567	ALS ICP-OES, MS	77.07	0.53	15.03	2.29	0.05	0.41	1.00	3.84	4.44	0.01	0.80	93.84	0.819	7.08	1.307	64	10	4.4	<5	<5	44	24.5	184	283	27.9	212	24.5	<2	<1	4	1.95	1127	7.4	1.9	1	2.8	21	19.98	3.5	44	81.8	12.43	49.9	9.03	2.55	8.44	1.21	7.48	1.47	4.29	0.64	4.23	0.64
H11-95	porphyritic rhyolite lava vitrophyre	Target Hill			Trv	No		35.971		39.50846	-115.97334	ALS ICP-OES, MS	76.01	0.13	12.82	1.47	0.06	0.21	1.30	2.61	5.40	0.01	1.79	90.12	0.875	8.01	1.026	8	<10	1.1	<5	<5	63	22.3	267	161	26.6	145	32.2	3	<1	4	7.59	465	5.4	2.9	1	0.7	31	25.52	9.22	34.4	63	7.17	26.1	6.19	0.79	4.73	0.74	4.47	0.84	2.39	0.33	2.13	0.31
H11-96	porphyritic rhyolite lava	Target Hill			Ttr	No		35.971		39.50817	-115.97438	ALS ICP-OES, MS	75.66	0.13	13.22	1.39	0.02	0.15	1.16	3.22	4.99	0.05	1.20	98.34	0.903	8.21	1.037	7	10	0.8	<5	<5	50	21	239	151	21.4	146	29.2	2	<1	4	3.86	455	5.3	2.6	1	0.8	28	25.73	5.15	35.4	61.6	7.18	26.4	6.13	0.79	4.8	0.7	4.18	0.72	2.06	0.28	1.83	0.25
H11-99	porphyritic rhyolite dome lava	Target Hill			Ttr	No		35.97	0.03	39.50146	-115.97250	ALS ICP-OES, MS	76.99	0.07	12.60	1.12	0.03	0.08	1.00	3.21	4.88	0.03	0.50	99.24	0.933	8.09	1.021	<5	<10	<0.5	<5	<5	40	20.3	237	117	19	99	26.3	2	<1	4	3.63	295	4.1	2.6	1	0.8	28	23.98	5.59	25.2	44.2	5.66	21.4	5.22	0.64	4.15	0.71	4.59	0.93	2.63	0.35	2.24	0.34
H10-106	porphyritic rhyolite	Mount Hope	crystalline		Trh	No		36.04	0.12	39.79245	-116.18489	WSU XRF	77.00	0.07	13.41	0.12	0.00	0.23	0.25	3.23	5.67	0.01		98.30	0.345	8.9	1.128	5	6	5	55	27	19	189	70	20	84	19.4		2	175			16											17.2	5.6	16	31		16													
H11-110	porphyritic rhyolite	west Garden Pass			Trv	Yes		36.05	0.04	39.83704	-116.19997	ALS ICP-OES, MS	73.06	0.02	13.24	1.82	0.09	0.19	2.33	3.52	4.45	1.28	1.70	98.96	0.905	7.97	0.995	<5	<10	<0.5	<5	<5	124	33.1	474	27	27.8	85	50.7	2	<1	13	19.6	65	5.5	5.4	1	1.9	55	27.08	5.35	13	27.3	3.44	13	4.83	0.12	4.58	0.83	5.27	0.9	2.25	0.3	1.94	0.24
H11-113	porphyritic rhyolite dike	east Garden Pass			Trd	Yes		35.98	0.04	39.82988	-116.19073	ALS ICP-OES, MS	75.86	0.01	13.67	1.19	0.10	0.03	0.71	4.01	4.31	0.09	0.60	98.73	0.975	8.32	1.098	<5	<10	<0.5	<5	<5	29	25.4	335	13	29.8	60	37.3	<2	<1	9	11.45	73	3.8	4	1	4.42	19.24	6.68	9.2	21.4	2.88	12.2	5.18	0.61	5.02	0.87	5.45	0.93	2.39	0.32	2.06	0.27
H11-129	porphyritic rhyolite dike	upper Windfall Canyon			Trd	No		35.8		39.45399	-115.98762	ALS ICP-OES, MS	74.71	0.06	12.96	1.13	0.03	0.11	3.81	1.09	6.07	0.03	4.99	94.90	0.911	7.16	NM	<5	<10	<0.5	<5	<5	77	21.2	289	71	28.2	109	32	2	<1	4	2.69	297	4.4	2.8	2	1.1	31	24.76	10.85	27.9	37.8	6.39	24	6.83	0.83	5.82	0.91	5.66	1.04	2.85	0.41	2.59	0.38
H11-130	porphyritic rhyolite dike	upper Windfall Canyon			Trd	No		35.86	0.05	39.46008	-115.98349	ALS ICP-OES, MS	79.27	0.06	13.00	1.41	0.07	0.06	0.15	1.01	4.94	0.02	2.50	95.75	0.959	5.95	NM	6	<10	0.5	<5	<5	57	21.2	257	55	26.8	97	28.6	2	<1	4	2.86	427	4.4	2.9	1	0.9	27	24.02	2.64	18.8	39.9	4.78	19.2	5.65	0.65	4.95	0.78	4.71	0.9	2.49	0.36	2.34	0.36
H11-131	porphyritic rhyolite dike	south of Pinto Basin			Trd	No		35.8		39.40747	-115.92039	ALS ICP-OES, MS	75.18	0.11	13.03	1.99	0.06	0.18	1.04	2.94	5.45	0.01	2.90	96.70	0.917	8.39	1.033	<5	<10	1	<5	<5	60	21.2	264	134	29.4	135	30.5	3	<1	6	6.14	496	4.7	3.4	1	0.7	31	27.3	10.45	31.4	58.4	6.74	24.7	5.85	0.67	4.9	0.8	5.01	0.95	2.81	0.37	2.65	0.39
H11-136	porphyritic rhyolite lava dome	Secret Canyon			Trd	No		35.98	0.04	39.39688	-115.95701	ALS ICP-OES, MS	75.07	0.40	15.53	1.51	0.01	0.45	0.49	1.36	5.04	0.13	4.19	97.24	0.770	6.4	NM	27	<10	2.9	<5	<5	68	24.4	234	119	20.7	267	31	<2	<1	4	4.57	1142	7.5	1.7	1	0.9	25	30.44	7.35	74	136.3	13.99	49.6	7.95	1.52	5.5	0.83	4.05	0.7	1.76	0.27	1.65	0.28
H11-139	porphyritic rhyolite dike	New York Canyon			Trd	No		35.8		39.46943	-115.97931	ALS ICP-OES, MS	80.88	0.07	13.30	1.23	0.04	0.09	0.14	0.89	3.34	0.01	5.28	93.59	0.932	4.23	NM	<5	<10	0.5	<5	<5	75	21.4	177	47	14.5	105	31.5	<2	<1	4	3.88	307	4.4	3.1	2	1.1	21	24.36	3.55	17.6	37	4.21	15.8	3.85	0.53	3.11	0.53	2.82	0.51	1.39	0.22	1.49	0.25
H11-140	porphyritic rhyolite dike	Dunderberg Mine			Trd	No		35.96	0.05	39.47732	-115.98065	ALS ICP-OES, MS	78.53	0.06	13.35	1.09	0.08	0.09	0.19	1.45	4.82	0.01	4.23	94.36	0.807	6.27	NM	<5	<10	0.5	<5	<5	58	21.9	256	58	15.8	104	31.6	<2	<1	4	4.59	279	4.3	3.1	2	1.5	26	25.12	6.08	19	29.6	4.78	18.5	4.62	0.68	3.6	0.61	3.17	0.57	1.5	0.23	1.58	0.25
H11-143	porphyritic rhyolite dike	Grey Fox Peak			Trd	No		35.78	0.07	39.39252	-115.96745	ALS ICP-OES, MS	76.32	0.12	12.65	1.64	0.03	0.16	0.90	3.13	5.01	0.02	1.00	97.61	0.911	8.14	1.038	6	<10	1	<5	<5	76	21.5	251	135	26.2	128	29	3	<1	5	5.27	598	4.5	3.7	1	0.9	31	28.38	6.3	43	76.3	8.92	31.7	6.33	0.75	5.04	0.82	4.58	0.87	2.41	0.35	2.21	0.34
H11-144	porphyritic rhyolite dike	upper Dale Canyon			Trd	No		35.7		39.42135	-115.96520	ALS ICP-OES, MS	78.70	0.29	14.04	1.63	0.03	0.36	0.29	0.62	3.93	0.10	4.31	96.19	0.819	4.55	NM	16	<10	1.7	<5	<5	49	22.9	206	77	26.6	216	27.2	<2	<1	5	6.22	1190	6.4	3	2	0.8	14	25.78	6.7	58.3	105	11.59	41	7.45	1.16	5.58	0.86	4.99	0.94	2.47	0.35	2.25	0.34
H11-216	porphyritic rhyolite dike	south of Lookout Mountain			Trd	No		35.7		39.40072	-115.99735	ALS ICP-OES, MS	74.37	0.44	15.30	2.48	0.02	0.68	0.87	1.44	4.26	0.15	6.99	91.17	0.785	5.7	NM	38	11	3.4	<5	<5	90	23.8	208	87	34.3	178	26.5	<2	<1	4	4.27	1048	5.4	2.9	1	18.3	24	23.36	7.1	45.6	87	9.61	35.1	7.29	1.37	6.45	1.03	5.93	1.15	3.12	0.45	2.71	0.42
H11-54B	porphyritic rhyolite pumice	Pinto Spring	vitrophyre		Tprt	No		36.6		39.43528	-115.92771	ALS ICP-OES, MS	76.76	0.04	13.15	0.89	0.09	0.05	0.83	3.50	4.68	0.01	3.69	96.92	0.947	8.18	1.067	<5	<10	<0.5	<5	<5	46	22.7	242	46	36.1	60	45	3	<1	5	6.65	59	3.1	4.3	3	0.8	34	27.13	10.63	11.3	24.5	3.21	12.3	4.63	0.33	5.59	0.95	6.23	1.21	3.42	0.51	3.18	0.45
H11-73	porphyritic rhyolite dome lava	near Sugarloaf			Tpr	No		36.6		39.40694	-115.95410	ALS ICP-OES, MS	76.96	0.02	13.97	1.05	0.02	0.16	0.30	2.83	4.62	0.08	2.30	94.86	0.868	7.45	1.382	<5	<10	<0.5	<5	<5	74	25	320	37	30	73	36.3	<2	<1	8	4.59	37	3.8	5.2	1	1.6	21	22.77	8.64	4.1	10.5	1.49	5.8	2.46	0.24	3.47	0.71	5.1	1.02	3.13	0.48	3.17	0.44
H11-79	porphyritic rhyolite lava dome	Pinto Peak dome			Tp	No		36.6		39.41543	-115.94778	ALS ICP-OES, MS	76.84	0.02	13.61	0.79	0.08	0.03	0.26	3.68	4.32	0.03	1.30	99.56	0.888	7.92	1.164	<5	<10	<0.5	<5	<5	42	25.1	326	17	46.7	54	59.6	<2	<1	13	6.86	42	3.7	6.1	2	1.4	23	28.12	7.58	15.6	33.2	4.02	16.7	4.76	0.42

Table 4: Summary of ore deposits in the map area.

Deposit	Easting (UTM NAD27)	Northing (UTM NAD27)	Metals and Recorded Production	Type	Description	References
Burning Moscow	586770	4365570	Ag-(Pb-Zn-Cu), unknown production	Polymetallic carbonate replacement	Replacement ore hosted by Eldorado dolomite, nearby jasperoid.	Nolan (1962); USGS MRDS database
Dugout Canyon	585440	4366750	Ag-Sb-Au-Zn-(Cu), 502 tons of valued at $42,503 during period of 1874–1936.	Polymetallic carbonate replacement	Ore in jasperoid cut by milky white quartz veins or in shattered dolomitized Pogonip Group limestones, locally abundant stibnite.	Nolan (1962); Couch and Carpenter (1943); USGS MRDS database; this study
Fairplay	601230	4362145	Ag-Pb-(Cu-Au), 2,265 tons of ore, 78,878 oz Ag, 325,853 lbs Pb, 7,987 lbs Cu, 6 oz Au, includes Queen	Polymetallic carbonate replacement	Mainly replacement ores, hosted by Hay Creek member of Devils Gate Limestone and dolomite of the Bay State member of the Nevada formation in the Alhambra Hills.	Nolan et al. (1974); Smith (1976)
4th of July	586880	4368250	Ag-Au-Pb-(Cu), one shipment of 1 ton @ 0.45 opt Au, 21.60 opt Ag, and 8.0% Pb	Polymetallic carbonate replacement	Mainly oxidized replacement ore, hosted by Hamburg dolomite in upper plate of Prospect Mountain thrust (Diamond Tunnel thrust); Workings from later Diamond Mine produced additional ore from lower levels.	Nolan (1962); USGS MRDS database
Geddes-Bertrand	587710	4363900	Ag-Pb-(Au),. 4,376 tons valued at $367,654 mined from 1873–1891. 1981–1985: 11,000 oz ag produced from ore that average 5 opt Ag	Polymetallic carbonate replacement	Gossanous replacement zones in Eldorado dolomite, local jasperoid.	Nolan et al (1974); Davis et al. (2006)
Hoosac	589200	4365680	Ag-Pb-Au-As, 17,292 tons of ore mine valued at $158,616 mined from 1872–1882.	Polymetallic carbonate replacement	Shear zones in Eureka Quartzite.	Nolan (1962); USGS MRDS database
Lookout Mountain	586170	4362800	Au-(As-Hg); 17,700 oz Au, 1987–1988; 2013 measured and indicated resource: 28,949,000 tons grading 0.018 ounces per ton, containing 508,000 ounces of gold	Carlin-type gold	Most of the ore occurs in a large hydrothermal collapse breccia along and in the footwall of the Lookout Mountain normal fault that places Devonian rocks against Cambrian rocks. The breccia formed by dissolution of carbonates in the Cambrian Hamburg dolomite, Dunderberg Shale, and to a much lesser extent in Devonian rocks. The breccia is variably silicified forming jasperoid. The ore is mostly oxidized. Unweathered ore in the Dunderberg shale is characterized by arsenian pyrite, arsenopyrite and realgar associated with quartz-kaolinite alteration. Coordinate is in the middle of Lookout Mountain pit, which is the main deposit of several deposits associated with large bodies of jasperoid that are aligned north-northwest over a distance of over 2 km on Ratto Ridge.	Timberline Resources (2013); this study
McCullough's Butte	578760	4363210	F-Be-Zn-(W-Mo-Sn-Ag), no reported production; old resource estimate of 110 million tons @ ~10% CaF_2	Polymetallic-fluorite skarn-vein	Zoned F-rich polyemetallic hydrothemral system associated with ~84 Ma 2-mica granitic intrusive complex. Zoned vein sequence from inner to outer: (1) pegmatitic quartz-feldspar-fluorite with greisen envelopes, (2) garnet-epidote-(quartz-fluorite-pyrite), (3) plagioclase-fluorite-muscovite-(quartz-sphalerite-molybdenite), (4) fluorite-muscovite-(calcite-dolomite-beryl-pyrite). Pogonip Group limestones are pervasively dolomitzed within that zoned system for a distance of almost 3 km from the outcrops of Cretaceous dikes. Widespread Ag-rich veins with quartz-calcite-dolomite-(barite-Sb-rich sulfosalts) on the edges of the system.	Barton (1982, 1987)
Oswego	587840	4362650	Au-(As-Ag), unknown production	Carlin-type gold	Disseminated gold ore in dolomite and shale along normal faults that place Secret Canyon Shale over Eldorado dolomite. Local orpiment and realgar.	Nolan et al (1974); Steininger et al. (1987).
Page and Corwin	589460	4362690	Ag-Pb-(Au), unknown production	Polymetallic carbonate replacement	Gossanous and silicified replacement zones in dolomitized Pogonip Group limestones; several prospects on north side of Round Top Mountain.	Nolan et al. (1974)
Queen	597700	4361900	Ag-Pb-(Cu-Au), 2,265 tons of ore, 78,878 oz Ag, 325,853 lbs Pb, 7,987 lbs Cu, 6 oz Au, includes Fairplay	Polymetallic carbonate replacement	Hosted in limestone and dolomite of Devils Gate Limestone. Mainly replacement ores on east side and high-grade Ag-Au quartz veins on the west side of Silverado Mountain.	Nolan et al. (1974); Smith (1976)
Reese and Berry	580200	4364570	Ag-	Polymetallic carbonate replacement	Brecciate Lone Mountain Dolomite with Ag-rich quartz-calcite-dolomite-(barite-stibnite-secondary Ag minerals, oxidized tetrahedrite) veins and breccia matrices; likely related to McCullough's Butte hydrothermal system	Barton (1982)
Rocky Canyon	585870	4364990	Mo-(W-F)	Molybdenum porphyry-skarn	Greisen veins with molybdenite and skarn associated with 86Ma two-mica granite porphyry dikes; only present in subsurface and intercepted by drill core	Barton (1987); this study
Windfall	588190	4367270	Au-(As-Hg); 1874-1951: 65,000 tons @ 0.368 opt for 23,920 oz Au; 1975–1989: ~90,000 oz Au;	Carlin-type gold	The gold ore occurred mainly in sanded (partially dedolomitized) Hamburg dolomite along its hanging wall contact with Dunderberg Shale, as well in jasperoid bodies in the Hamburg. Ore is mostly oxidized, but when unweathered is associated with fine-grained pyrite and local realgar (mainly in the Dunderberg) and contained high concentrations of arsenic and mercury. The pits were aligned north-northwest along the Hamburg-Dunderberg contact, spaced over a distance of 2.3 km. Highest grades were along Ne-trending faults that crossed the contact. Coordinate is from the middle of the Windfall pit.	Nolan (1962); Wilson and Wilson (1986); this study